

Diagnostic Performance of In-Procedure Angiography-Derived Quantitative Flow Reserve Compared to Pressure-Derived Fractional Flow Reserve: The FAVOR II Europe-Japan Study

Jelmer Westra, BSc; Birgitte Krogsgaard Andersen, BSc; Gianluca Campo, MD; Hitoshi Matsuo, MD, PhD; Lukasz Koltowski, MD; Ashkan Eftekhari, MD, PhD; Tommy Liu, MD; Luigi Di Serafino, MD, PhD; Domenico Di Girolamo, MD; Javier Escaned, MD, PhD; Holger Nef, MD, PhD; Christoph Naber, MD, PhD; Marco Barbierato, MD; Shengxian Tu, PhD; Omeed Neghabat, BSc; Morten Madsen, MSc; Matteo Tebaldi, MD; Toru Tanigaki, MD; Janusz Kochman, MD; Samer Somi, MD, PhD; Giovanni Esposito, MD, PhD; Giuseppe Mercione, MD; Hernan Mejia-Renteria, MD; Federico Ronco, MD; Hans Erik Bøtker, MD, PhD; William Wijns, MD, PhD; Evald Høj Christiansen, MD, PhD; Niels Ramsing Holm, MD

Background—Quantitative flow ratio (QFR) is a novel modality for physiological lesion assessment based on 3-dimensional vessel reconstructions and contrast flow velocity estimates. We evaluated the value of online QFR during routine invasive coronary angiography for procedural feasibility, diagnostic performance, and agreement with pressure-wire-derived fractional flow reserve (FFR) as a gold standard in an international multicenter study.

Methods and Results—FAVOR II E-J (Functional Assessment by Various Flow Reconstructions II Europe-Japan) was a prospective, observational, investigator-initiated study. Patients with stable angina pectoris were enrolled in 11 international centers. FFR and online QFR computation were performed in all eligible lesions. An independent core lab performed 2-dimensional quantitative coronary angiography (2D-QCA) analysis of all lesions assessed with QFR and FFR. The primary comparison was sensitivity and specificity of QFR compared with 2D-QCA using FFR as a reference standard. A total of 329 patients were enrolled. Paired assessment of FFR, QFR, and 2D-QCA was available for 317 lesions. Mean FFR, QFR, and percent diameter stenosis were 0.83 ± 0.09 , 0.82 ± 10 , and $45 \pm 10\%$, respectively. FFR was ≤ 0.80 in 104 (33%) lesions. Sensitivity and specificity by QFR was significantly higher than by 2D-QCA (sensitivity, 86.5% (78.4–92.4) versus 44.2% (34.5–54.3); $P < 0.001$; specificity, 86.9% (81.6–91.1) versus 76.5% (70.3–82.0); $P = 0.002$). Area under the receiver curve was significantly higher for QFR compared with 2D-QCA (area under the receiver curve, 0.92 [0.89–0.96] versus 0.64 [0.57–0.70]; $P < 0.001$). Median time to QFR was significantly lower than median time to FFR (time to QFR, 5.0 minutes [interquartile range, –6.1] versus time to FFR, 7.0 minutes [interquartile range, 5.0–10.0]; $P < 0.001$).

Conclusions—Online computation of QFR in the catheterization laboratory is clinically feasible and is superior to angiographic assessment for evaluation of intermediary coronary artery stenosis using FFR as a reference standard.

Clinical Trial Registration—URL: <https://www.clinicaltrials.gov>. Unique identifier: NCT02959814. (*J Am Heart Assoc.* 2018;7:e009603. DOI: 10.1161/JAHA.118.009603.)

Key Words: fractional flow reserve • quantitative coronary angiography

From the Departments of Cardiology (J.W., B.K.A., A.E., O.N., H.E.B., E.H.C., N.R.H.), Clinical Epidemiology (M.M.), Aarhus University Hospital, Skejby, Denmark; Cardiovascular Institute, Azienda Ospedaliero-Universitaria di Ferrara, Cona, Italy (G.C., M.T.); Maria Cecilia Hospital, GVM Care and Research, Cotignola (RA), Italy (G.C.); Department of Cardiovascular Medicine, Gifu Heart Center, Gifu City, Japan (H.M., T.T.); Department of Cardiology, Medical University of Warsaw, Warszawa, Poland (L.K., J.K.); Department of Cardiology, Hagaziekenhuis, The Hague, The Netherlands (T.L., S.S.); Division of Cardiology, Department of Advanced Biomedical Sciences, University of Naples Federico II, Naples, Italy (L.D.S., G.E.); Azienda Ospedaliera Sant'Anna e San Sebastiano, Caserta, Italy (D.D.G., G.M.); Hospital Clinico San Carlos IDISSC, Complutense University, Madrid, Spain (J.E., H.M.-R.); Department of Cardiology and Angiology, University of Giessen, Giessen, Germany (H.N.); Klinik für Kardiologie und Angiologie, Essen, Germany (C.N.); Emodinamica Aziendale AULSS 3 Serenissima, Ospedale Dell'Angelo, Mestre, Italy (M.B., F.R.); School of Biomedical Engineering, Shanghai Jiao Tong University, Shanghai, China (S.T.); The Lambe Institute for Translational Medicine and Curam, National University of Ireland Galway, Galway, Ireland (W.W.). Accompanying Data S1, S2, Tables S1 through S6 and Figures S1 through S11 are available at <http://jaha.ahajournals.org/content/7/14/e009603/DC1/embed/inline-supplementary-material-1.pdf>

Correspondence to: Niels Ramsing Holm, MD, Department of Cardiology, Aarhus University Hospital, Skejby, Palle Juul-Jensens Boulevard 99, 8200 Aarhus N, Denmark. E-mail: niels.holm@clin.au.dk

Received April 29, 2018; accepted June 1, 2018.

© 2018 The Authors. Published on behalf of the American Heart Association, Inc., by Wiley. This is an open access article under the terms of the Creative Commons Attribution License, which permits use, distribution and reproduction in any medium, provided the original work is properly cited.

Clinical Perspective

What Is New?

- Quantitative flow ratio (QFR) estimates fractional flow reserve based on computation of 2 standard angiographic projections.
- Online QFR performed during invasive angiography is feasible and can be computed within the time of conventional fractional flow reserve measurement.
- QFR has superior sensitivity and specificity for detection of functional significant lesions in comparison with 2-dimensional quantitative coronary angiography using fractional flow reserve as reference.

What Are the Clinical Implications?

- QFR may broaden the access to physiological lesion assessment in diagnostic catheterization laboratories and centers with low adoption of pressure-wire–based diagnostic strategies.
- Randomized trials are required to confirm that QFR provides noninferior clinical outcome compared to assessment of intermediate coronary stenosis by pressure wire.

Physiological assessment is the clinical standard to guide percutaneous coronary interventions of intermediate coronary stenosis. Following the FAME (Fractional Flow Reserve Versus Angiography for Multivessel Evaluation [fractional flow reserve versus angiography for guiding percutaneous coronary intervention]) trials, the adoption of fractional flow reserve (FFR) has improved with a 16-fold increase in FFR-guided percutaneous coronary intervention in the United States from 2008 to 2012.¹ Globally, the use of physiological lesion assessment remains low, with large areas performing less than 15% of eligible procedures with physiology guidance.^{2,3}

To further expand the use of physiological-guided percutaneous coronary intervention, coronary computed tomography angiography– and invasive coronary angiography–based computation methods were developed for less-invasive FFR approximation.^{4–10}

Quantitative flow ratio (QFR) is a method for fast computation of FFR based on 3-dimensional quantitative coronary angiography (3D-QCA) and estimation of contrast flow velocity during invasive coronary angiography. The optimal approach was validated in the FAVOR (Functional Assessment by Various Flow Reconstructions) multicenter study, proving that QFR can be computed without pharmacology-induced hyperemia.¹¹ In FAVOR, QFR was computed post hoc in a core-lab setting. The FAVOR II China study, conducted in parallel to FAVOR II Europe-Japan (E-J), showed a high diagnostic accuracy of in-procedure QFR.¹²

In FAVOR II E-J, we aimed to validate the in-procedure feasibility and compare the diagnostic performance of QFR computation with 2-dimensional quantitative coronary angiography (2D-QCA) in a multicenter setting, using FFR as a reference standard.

Methods

Study Design

FAVOR II E-J was a prospective, blinded, observational study with paired assessment of QFR, 2D-QCA, and FFR performed at 11 international sites: Italy (4), The Netherlands (1), Germany (2), Poland (1), Spain (1), Japan (1), and Denmark (1). Clinicaltrials.gov identifier: NCT02959814.

Primary Comparison

The primary comparison was sensitivity and specificity of QFR compared with 2D-QCA to detect hemodynamically significant coronary lesions with FFR as a gold standard. For FFR and QFR, significant obstructions were defined as FFR and QFR ≤ 0.80 whereas $>50\%$ diameter stenosis (% DS) was used for 2D-QCA. Sample-size calculation and a full list of secondary comparisons are provided in Data S1 and Table S1.

Patient Population

Patients with stable angina pectoris or patients scheduled for secondary evaluation of stenosis after acute myocardial infarction were eligible for enrollment when the angiographic inclusion criteria were met; indication for FFR measurement (at least 1 lesion with % DS 30–90 in a vessel with reference size >2.0 mm). Exclusion criteria were: acute myocardial infarction within 72 hours; severe asthma or severe chronic obstructive pulmonary disease; allergy to contrast media or adenosine; or atrial fibrillation. All inclusion and exclusion criteria are listed in Table S2.

Ethics

The study was approved by the Central Denmark Region Committees on Biomedical Research Ethics. Approval by local or national medical ethics committees was obtained by the local or national coordinating investigators as required for the individual sites. The Danish Data Protection Agency approved the study. All enrolled patients provided written informed consent. J.W. and N.R.H. had full access to all data in the study. All authors are responsible for integrity of the analysis. The data will not be made available to other researchers for purposes of reproducing the results or replication the procedure because of competitive reasons.

Study Procedure

Invasive coronary angiography

Nitroglycerine (100–200 μg IC) was administered after acquiring the first angiographic projection. If FFR was indicated in 1 or more vessels, 2 study projections were obtained for each lesion of interest at a minimum of 12.5 frames per second. Selection of projections aimed for minimal vessel foreshortening and minimal vessel overlap by: (1) brisk, continuous and fast contrast injections and (2) no zooming and movement of the table and visualization of the entire vessel to the intended location of the pressure transducer. A table of recommended projection angles was provided for all study sites (Table S3). Images were transferred to a workstation for computation of QFR following site-specific blinding protocols (Data S1). The remaining diagnostic invasive coronary angiography and further interventions were performed per normal clinical practice.

QFR computation

QFR was computed with the CE-marked software; QAngio XA-3D/QFR solution (Medis medical imaging system bv., Leiden, The Netherlands). An end-diastolic frame was selected for each study projection and was used for the 3-dimensional reconstruction of the segmented vessel. The reference vessel was constructed by fitting to healthy segments preferably proximal and distal to the lesion of interest. The following quality checks of the reference vessel reconstruction were performed: vessel tapering; good correspondence between the 2 images used for reconstruction; the reference should not follow aneurysmatic sections; and realistic proximal sizing per sex and race. The contrast frame count was performed in an angiographic run with contrast movement clearly visualized and preferably with frames from the same cardiac cycle.¹³ The detailed standard operating procedure for QFR computation is presented in Data S2. All analyses were repeated in a core-lab setting (CardHemo, Med-X Research Institute, Shanghai Jiao Tong University, Shanghai, China). Frame count based contrast-QFR was used for all analysis.

FFR measurement

FFR was measured according to current guidelines.¹⁴ Volcano (San Diego, CA) or Abbott (Abbott Park, IL) pressure wires were used. Hyperemia was induced using intravenous adenosine (femoral or brachial vein infusion of adenosine at 140 $\mu\text{g}/\text{L}/\text{min}$) or intracoronary adenosine (100 μg [right coronary artery] or 200 μg [left coronary artery]). The pressure transducer location was documented angiographically for all measurements. A drift-value within the range of 0.04 was accepted; otherwise, the procedure was repeated. For FFR values of 0.76 to 0.84, a drift value not exceeding 0.02 was required.

Core-Lab Waveform Analysis

FFR waveform analysis was performed at the Institute of Clinical Medicine, Aarhus University, Denmark. The observer was blinded to clinical and procedural information. Exclusion of cases with nonanalyzable FFR waveforms required massive dampening, no identification of a stable distal pressure/aortic pressure ratio during hyperemia (identical value in the same phase of the cardiac cycle over 3 beats), no drift measurement, or loss of distal pressure or aortic pressure.

Continuous Feedback

During the enrollment period, all sites received day-to-day feedback from the QFR and FFR core labs on image acquisition quality, pressure wave-form quality, and adherence to the standard operating procedure for QFR analysis.

Statistical Analysis

Baseline characteristics and procedural characteristics were presented as count and percentages, continuous variables as mean and SD, if normally distributed, or otherwise reported as medians and interquartile range. Feasibility was calculated as the fraction of successful QFR computations of lesions with successful FFR measurements. The primary comparison was calculated as superiority for sensitivity and specificity of QFR (in-procedure value) in comparison with 2D-QCA (Table S1). Sensitivity and specificity for 2D-QCA and QFR were compared using McNemar's test. Negative predictive value, positive predicate value, positive likelihood ratio, and negative likelihood ratio for 2D-QCA and QFR were compared using generalized score statistics. Time to FFR and QFR were compared using Wilcoxon's rank test. The diagnostic performance of QFR compared with 2D-QCA was assessed by 2-tailed paired comparison of receiver operating characteristics curves (DeLong's method). Pearson's correlation was used to quantify the correlation between QFR and FFR. Agreement between QFR and FFR was assessed by Bland–Altman plots. Observations in patients with more than 1 study vessel were presumed independent. This assumption was evaluated by repeated analysis on a per-patient level. If multiple measurements were performed, the lowest FFR and corresponding QFR and % DS (2D-QCA) values were compared with per-patient analysis. Reproducibility was assessed as interobserver variation by Bland–Altman and scatter analysis of in-procedure QFR and core-lab QFR. The diagnostic performance of core-lab QFR compared with in-procedure QFR was assessed by 2-tailed paired comparison of receiver operating characteristics curves (DeLong's method) using FFR as a reference. Subgroup analysis for QFR accuracy was performed per FFR strata, per vessel, and for single versus tandem lesions. The diagnostic performance of 3-dimensional

quantitative coronary angiography–derived % DS and area stenosis was compared with QFR with FFR as a reference standard using receiver operating characteristics curves (DeLong’s method). Analysis was performed using STATA (version 13; StataCorp LP, College Station, TX) and R software (R Foundation for Statistical Computing, Vienna, Austria).

Results

Three hundred twenty-nine patients were included from February 22, 2017 to October 17, 2017 (Table S4). In-procedure QFR was computed in 345 (96%) vessels with successful FFR measurements. After exclusion based on predefined FFR core-lab criteria, 272 patients and 317 vessels were included in the final analysis (patient flow chart in Figure 1 and vessel-level flow chart in Figure S1). Mean FFR was 0.83 ± 0.09 (Figure S2), and mean % DS (2D-QCA) was $45 \pm 10\%$. An FFR ≤ 0.80 was found in 104 (33%) vessels. Baseline and procedural characteristics are listed in Tables 1 and 2.

Diagnostic Performance of QFR and 2D-QCA

Sensitivity and specificity of QFR were significantly higher than of 2D-QCA 50% DS with FFR as a reference (sensitivity, 86.5% [95% confidence interval {CI}, 78.4–92.4] versus 44.2% [95% CI, 34.5–54.3]; $P < 0.001$ and specificity, 88.9% [95% CI, 81.6–91.1] versus 76.5% [95% CI, 70.3–82.9];

$P = 0.002$; Figure 2). Overall diagnostic accuracy was significantly higher for QFR compared with 2D-QCA 50% DS using FFR ≤ 0.80 as a reference (86.8% versus 65.9%; $P < 0.001$; Table S5). Area under receiver curve (AUC) was larger for QFR compared with 2D-QCA with FFR as a reference (AUC, 0.92 [95% CI, 0.89–0.95] versus 0.64 [95% CI, 0.57–0.70]; $P < 0.001$; Figure 3). QFR was also superior on a per-patient level (sensitivity, 83.5% [95% CI, 74.9–90.1] versus 40.8% [95% CI, 31.2–50.9]; $P < 0.001$; specificity, 83.4% [95% CI, 77.0–88.7] versus 74% [95% CI, 66.7–80.4]; $P = 0.03$; and AUC, 0.91 [95% CI, 0.87–0.94] versus 0.60 [95% CI, 0.53–0.67]; $P < 0.001$; Figure S3). Additional results of diagnostic comparisons are listed in Table 3.

Correlation and Agreement

QFR showed per-vessel correlation ($r = 0.83$; $P < 0.001$) and agreement (mean difference, 0.01 ± 0.06) with FFR (Figure 4). QFR showed per-patient correlation ($r = 0.80$; $P < 0.001$) and agreement (mean difference, 0.01 ± 0.07 ; Figure S4).

Time to FFR and QFR

Paired assessment of time to QFR and FFR was available for 295 lesions (93%). Time to completed QFR was significantly shorter than time to completed FFR (median time to QFR, 5.0 minutes [interquartile range, 3.5–6.1] versus median time to FFR 7.0 minutes [interquartile range, 5.0–10.0]; $P < 0.001$; Figure 5).

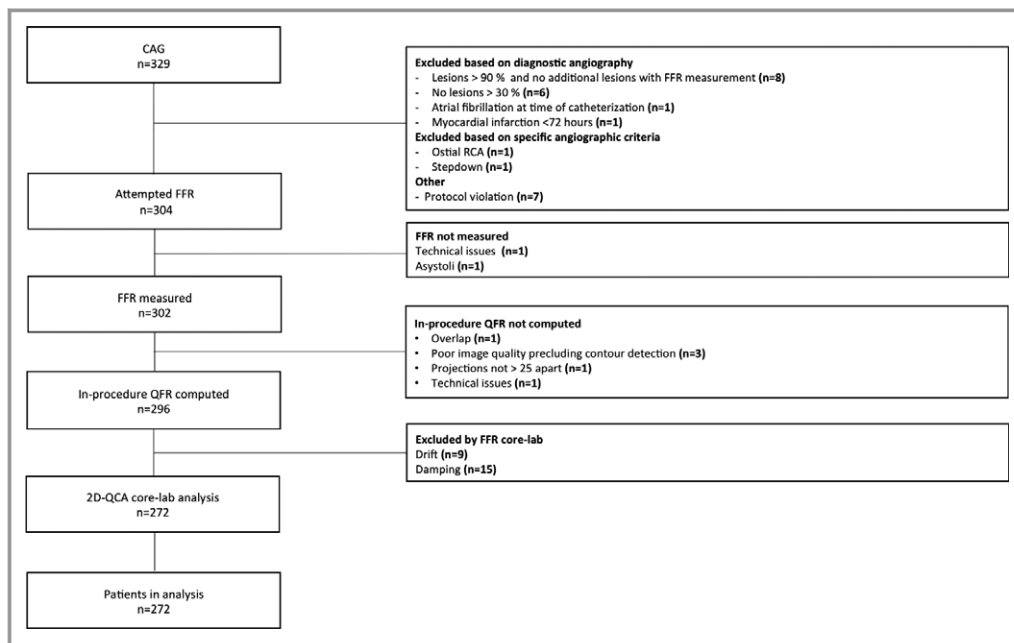


Figure 1. Study enrollment flow chart. FFR indicates fractional flow reserve; N, number of patients; QCA, quantitative coronary angiography; QFR, quantitative flow ratio; RCA, right coronary artery.

Table 1. Baseline Characteristics

Baseline Characteristics (n=272)	
Clinical	
Age, y	67±10
Male	196 (72%)
Smoking (current or past)	156 (57%)
BMI, kg/m ²	27±5
Hypertension	201 (74%)
Hyperlipidemia	186 (68%)
Diabetes mellitus	78 (29%)
Family history of CAD	73 (27%)
Ejection fraction, %	56±10
Previous PCI	109 (40%)
Previous CABG	11 (4%)
Clinical presentation	
CCS 0	54 (20%)
CCS I	67 (25%)
CCS II	122 (45%)
CCS III	14 (5%)
CCS IV	1 (0%)
Acute myocardial infarction	6 (2%)
Other (dyspnea, arrhythmia)	8 (3%)
Procedure characteristics	
Procedure time, min	43±30
Flouro time, min	10±7
Contrast use, mL	118±72

Data presented as n (%) or mean±SD. BMI indicates body mass index; CABG, coronary artery bypass surgery; CAD, coronary artery disease; CCS, Canadian Cardiovascular Society grading of angina pectoris; PCI, percutaneous coronary interventions.

Reproducibility

Core-lab analysis showed per-vessel correlation ($r=0.73$; $P<0.001$) and agreement (mean difference, -0.01 ± 0.06) for QFR and FFR (Figure S5). We found no statistically significant difference in per-patient AUC for in-procedure QFR and core-lab QFR measurements (Figure S6). Comparison of in-procedure QFR and core-lab QFR revealed correlation ($\rho=0.83$; $P<0.001$) and agreement (mean difference, -0.03 ± 0.07 ; Figure S7).

Hybrid Model Limits

QFR limits to yield specificity and sensitivity >95% with FFR as a reference were 0.77 (QFR-treat) and 0.87 (QFR-defer). Applying the 95% limits to this sample, use of pressure wires and adenosine could theoretically have been avoided in 64% of all measurements yielding 95% accuracy with FFR as a reference standard (Figure S8). Applying a 100% limit (QFR-

Table 2. Lesion Characteristics

Vessel Characteristics (n=317)	
Vessel	
Left main coronary artery	4 (1%)
Left anterior descending artery	160 (50%)
Diagonal branch	5 (1%)
Left circumflex artery	50 (16%)
Obtuse marginal branch	23 (7%)
Ramus intermedius	3 (1%)
Right coronary artery	68 (22%)
Posterior descending artery	2 (1%)
Posterolateral branch	2 (1%)
Anatomy	
Diameter stenosis, %	45±10
Minimal lumen diameter, mm	1.57 (IQR, 1.27–1.90)
Reference diameter, mm	2.82 (IQR, 2.44–3.20)
Minimal lumen area, mm ²	1.93 (IQR, 1.26–2.84)
Lesion length, mm	9.64 (IQR, 7.53–13.76)
Tandem lesions	124 (39%)
Calcified vessels	41 (13%)
Tortuous vessels	34 (11%)
Physiology	
FFR	0.83±0.09
FFR ≤0.80	104 (33%)
FFR 0.75 to 0.85	101 (32%)

Data are presented as n (%) or mean±SD. FFR indicates fractional flow reserve; IQR, interquartile range.

treat 0.64 and QFR-defer 0.93) to this sample, pressure wires and adenosine theoretically were not required in 21% of measurements yielding 100% accuracy with FFR as a reference standard. This analysis assumes that FFR is 100% accurate. The trade-off for pressure-wire-free procedures depending on aimed accuracy with FFR as a reference is illustrated in Figure S9.

Subgroup Analysis

The precision (absolute difference of QFR-FFR) for QFR with FFR as a reference was not different across strata of FFR values (0.06 for FFR, 0.55–0.64; 0.07 for FFR, 0.65–0.74; 0.04 for FFR, 0.75–0.84; and 0.04 for FFR, ≥0.85; $P=0.47$). Diagnostic accuracy was significantly reduced for lesions, with FFR 0.75 to 0.84 (was 100% for FFR 0.55–0.64; 92.7% for FFR 0.65–0.74; 71.3% for FFR 0.75–0.84; and 93.9% for FFR ≥0.85; $P<0.001$). We found no statistically significant difference in precision of QFR (absolute difference QFR-FFR)

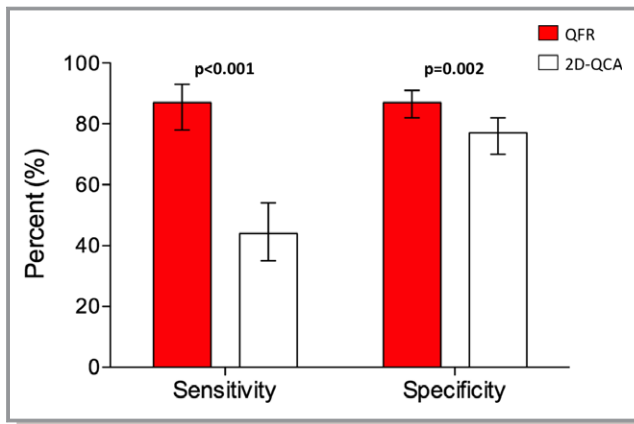


Figure 2. Sensitivity and specificity for QFR and 2D-QCA with FFR as reference. QFR was superior to 2D-QCA on sensitivity and specificity with FFR as reference standard. Diagnostic cutoffs: ≤ 0.80 for FFR and QFR; $\geq 50\%$ DS for 2D-QCA. 2D-QCA indicates 2-dimensional coronary angiography; QFR, quantitative flow ratio.

per vessel ($P=0.33$) nor for tandem lesions versus single lesions ($P=0.51$). QFR was superior to 3-dimensional quantitative coronary angiography diameter stenosis (AUC, 0.92 [95% CI, 0.89–0.95] versus 0.74 [95% CI, 0.69–0.80]; $P<0.001$) and 3-dimensional quantitative coronary angiography area stenosis (AUC, 0.92 [95% CI, 0.89–0.95] versus 0.62 [95% CI, 0.55–0.69]; $P<0.001$; Figure S10). Diabetes mellitus showed statistical significant association with increased QFR-FFR discrepancy (Table S6).

Discussion

The FAVOR II E-J study and the FAVOR II China study were the first multicenter studies investigating the feasibility and value of in-procedure QFR calculated in the catheterization

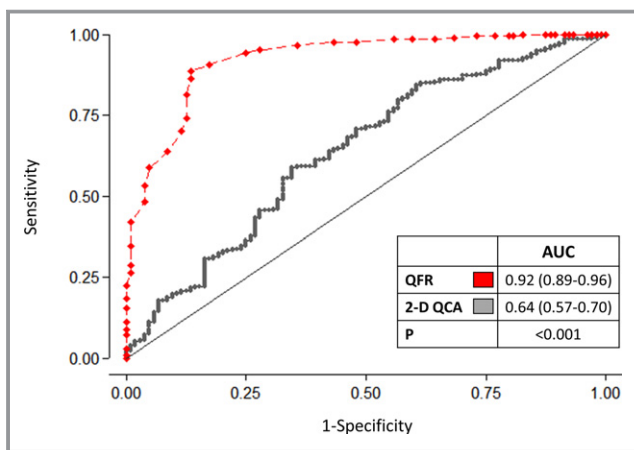


Figure 3. Per-vessel level diagnostic performance. FFR ≤ 0.80 was used as reference. 2D-QCA indicates 2-dimensional coronary angiography; AUC, area under the receiver operating curve; QFR, quantitative flow ratio.

Table 3. Diagnostic Performance

	QFR	2D-QCA	P Value
Accuracy	86.8%	65.9%	<0.001
AUC	0.92 (0.89–0.96)	0.64 (0.57–0.70)	<0.001
Sensitivity	86.5 (78.4–92.4)	44.2 (34.5–54.3)	<0.001
Specificity	86.9 (81.6–91.1)	76.5 (70.3–82.0)	0.002
PPV	76.3 (67.6–83.6)	47.9 (37.6–58.4)	<0.001
NPV	93.0 (88.5–96.1)	73.8 (67.4–79.4)	0.001
LR (+)	6.58 (4.62–9.37)	1.88 (1.36–2.61)	<0.001
LR (–)	0.16 (0.09–0.25)	0.73 (0.61–0.88)	0.001

Comparison of QFR and 2D-QCA with FFR as reference. Diagnostic cut-offs: ≤ 0.80 for FFR and QFR; $\geq 50\%$ DS for 2D-QCA. 2D-QCA indicates two-dimensional quantitative coronary angiography; LR (–), negative likelihood ratio; LR (+), positive likelihood ratio; NPV, negative predictive value; PPV, positive predictive value; QFR, quantitative flow ratio.

laboratory. The main findings of FAVOR II E-J were: (1) The study confirmed the primary hypothesis with superior specificity and sensitivity of QFR compared with standard anatomical assessment by 2D-QCA with FFR as a reference standard, and (2) QFR was feasible in a multicenter setting and was faster than FFR when analyzed during coronary angiography.

Diagnostic performance of QFR in FAVOR II E-J was noteworthy and comparable with the findings in the recent and almost similar FAVOR II China study.¹² SDs for mean difference FFR-QFR were identical (0.06). The higher accuracy (92.7%) in FAVOR II China may be explained by the smaller number of lesions with FFR values close to the FFR 0.80 cutpoint. Results in both studies showed improved performance of QFR compared with early validation studies on offline computation of QFR.^{11,15} The improved precision may be facilitated by the online analysis setup with instant feedback between operator and analyst. The standard operating procedure (Data S2), use of recommended angulations for angiographic projections (Table S3), and day-to-day feedback on enrolled cases may further have contributed to the improved results of QFR.

Most existing FFR computation methods for invasive coronary angiography predominantly rely on computational fluid dynamics.^{5,6,16} Inherited limitations of these methods may exist related to generating theoretical boundary conditions to create a “one-size-fits-all”, and to long computation time for blood flow simulations. Morris et al recently presented a rapid computational fluid dynamics modality for calculation of virtual FFR with a high diagnostic precision (100% for FFR ≤ 0.80) and short mean time to virtual FFR (189 seconds).¹⁷ This study was performed using rotational angiography in a limited population of 20 patients. To our knowledge, the FAVOR II studies using QFR present the first data supporting that real-time computation of FFR is feasible,

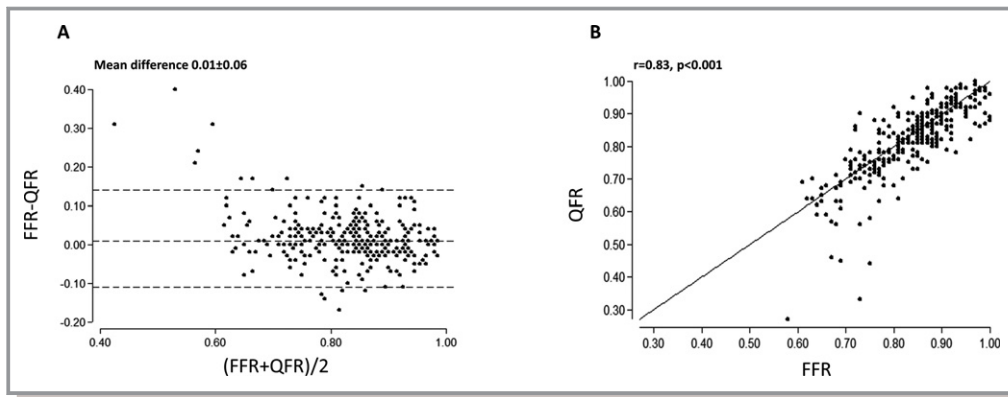


Figure 4. Agreement between QFR and FFR. A good correlation (A) and agreement (B) of QFR and FFR was observed. Dashed lines in Bland–Altman plot illustrate mean difference ± 2 SD. FFR indicates fractional flow reserve; QFR, quantitative flow ratio.

fast, and accurate in patients with stable angina pectoris and applicable stenosis.

FFR is the established standard for invasive identification of flow limiting intermediate coronary lesions when no other objective evidence of lesion specific ischemia is present.¹⁸ The clinical adaption of FFR is increasing, but remains low.^{1,2,19} The underlying reasons may include the high cost of pressure wires, tortuous vessels, and the need for pharmacological hyperemia induction. Multiple studies presented approaches to avoid hyperemia for physiological lesion assessment, such as instantaneous wave-free ratio and resting distal pressure/aortic pressure measurements. The resting indices perform similar with an overall diagnostic agreement between 80% and 90% when compared with FFR depending on distribution of lesions included in the studies.^{20–24} Still, instantaneous wave-free ratio–based strategies versus an FFR strategy resulted in comparable clinical outcomes at 1 year in 2 large, randomized clinical trials.^{23,24} We found a diagnostic accuracy for QFR (87%)

comparable to the early instantaneous wave-free ratio/FFR studies. Hence, the presented results support future comparison of FFR and QFR in clinical outcome trials.

Repeated core-lab QFR analysis confirmed the agreement between QFR and FFR (identical SD of 0.06). However, direct comparison of in-procedure QFR and core-lab QFR revealed a small bias. The discrepancy indicates that the standard operating procedure for QFR computation might not have been sufficiently standardized for some lesion presentations or training was insufficient before study start. Core-lab QFR showed less variation in disagreement at lower FFR values (Figure S5), indicating that contouring tight lesions could pose a specific challenge. Computation of QFR requires user interaction at steps, such as frame selection, lumen contouring, and contrast flow evaluation, and may hence be sensitive to small differences in the approach at various steps. A more elaborate standard operating procedure, more observer training, and automatizations are likely to reduce variation.

We showed that QFR is superior to standard quantitative coronary angiography in evaluating coronary artery stenosis. QFR may extend the access to physiology-based guidance when access to pressure wires is limited by financial restrictions or inexpedient reimbursement systems. By enrolling patients where FFR is normally indicated, we included a distribution of lesions with a mean FFR approaching the clinical 0.80 cutpoint (mean FFR, 0.83 ± 0.09). The vast majority of binary mismatches (treat/no-treat) between QFR and FFR were cases close to the binary diagnostic cutoff, in whom the benefit of treatment approaches the percutaneous coronary intervention–related event rate.²⁵ Although the study was not powered to do so, the sample allowed for the predefined assessment of a QFR-FFR hybrid approach, which may reflect the true clinical application of QFR in centers with full adoption of physiology-based diagnostics awaiting results of randomized outcome trials. Applying the 95% QFR-hybrid limits (QFR-treat 0.77 and QFR-defer 0.86) to

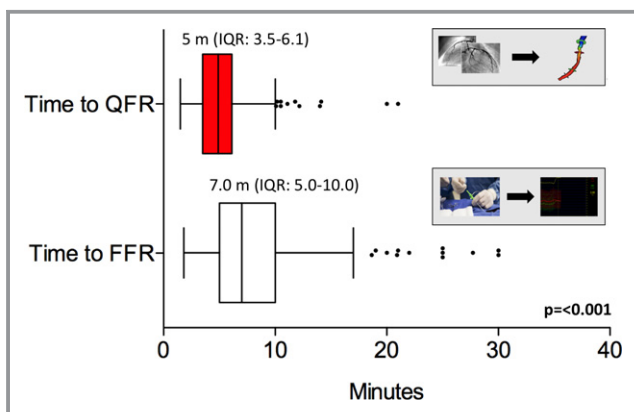


Figure 5. Comparison of time to FFR and time to QFR. FFR indicates fractional flow reserve; IQR, inter quartile range; m, minutes; QFR, quantitative flow ratio.

this population could potentially save pressure wires and adenosine in 64% of all lesions (Figure S8) and still ensure a diagnostic quality at the level of full FFR evaluation until clinical noninferiority of a QFR-based diagnostic strategy has been established.

Study Limitations

We only enrolled a limited portion of patients scheduled for secondary evaluation of coronary lesions after myocardial infarction. The diagnostic precision of QFR in nonculprit lesions, as recently assessed in a proof concept study by Spitaleri et al, could thus not be confirmed.²⁶ We excluded lesions with Medina type 1.1.1 and 1.0.1 bifurcations attributed to specific limitations of the present QFR application; hence, the diagnostic precision of QFR in bifurcation needs further developments and investigation. Despite the inclusion of tandem lesions, we did not mandate FFR-pullbacks during intravenous adenosine. Thus, a direct comparison between the FFR-pullback curves and the spatially sensitive, color-coded, continuous QFR values along the 3-dimensional/angiographic roadmap could not be performed. Because FFR was the sole gold-standard, we were not able to further characterize the lesion physiology in the presence of microvascular dysfunction. Time to QFR did not include the time for angiographic acquisition that could differ from an FFR-based strategy. It is therefore not possible to determine whether use of the provided standard projections and requirement for limited overlap and foreshortening added procedure time. To emulate an integrated QFR solution, data transfer time from angiographic equipment to the QFR workstation was not included in time to QFR. In case of selection of a different view during analysis, the additional time was included in the time to QFR. Furthermore, preparing and zeroing the pressure system was not included in time to FFR because of site-specific differences in the workflow.

Conclusion

In-procedure QFR is clinically feasible and is superior to angiographic assessment for evaluation of intermediary coronary artery stenosis when FFR is used as a reference. QFR bears the potential to expand the adoption of physiological lesion assessment.

Acknowledgments

All authors thank Joan Tuinenburg and Rolf Kooistra for their contribution to the 2D-QCA analysis and Yimin Zhang, Yunxiao Zhang for their contribution to the QFR core lab analysis. Westra acknowledges the support from Aarhus University (PhD scholarship).

Sources of Funding

The study was funded by the Department of Cardiology, Aarhus University Hospital, Skejby and by the participating institutions. The manufacturer and distributor of the QFR software (Medis Medical Imaging bv., Leiden, NL) was not involved in design, conduct, or reporting of the study and provided no funding for the study except for making the Medis Suite solution available for free in the study period and provided training for participating sites.

Disclosures

Westra received travel support and consultant fees from Medis Medical Imaging systems bv. Shengxian Tu received research from Medis Medical imaging systems bv. and Pulse medical imaging technology. Wijns received research grants (to his former institution) from stent manufacturing companies and speaker fees and honoraria from Biotronik, Mi-Cell, and MicroPort. He is a co-founder of Argonauts, an innovation facilitator. His research is supported by Science Foundation Ireland (Dublin). Holm received institutional research grants from Abbott, Boston Scientific, and Medis medical imaging. The remaining authors have no disclosures to report.

References

- Pothineni NV, Shah NS, Rochlani Y, Nairooz R, Raina S, Leesar MA, Uretsky BF, Hakeem A. U.S. trends in inpatient utilization of fractional flow reserve and percutaneous coronary intervention. *J Am Coll Cardiol*. 2016;67:732–733.
- Gotberg M, Cook CM, Sen S, Nijjer S, Escaned J, Davies JE. The evolving future of instantaneous wave-free ratio and fractional flow reserve. *J Am Coll Cardiol*. 2017;70:1379–1402.
- Toth GG, Toth B, Johnson NP, De Vroey F, Di Serafino L, Pyxaras S, Rusinaru D, Di Gioia G, Pellicano M, Barbato E, Van Mieghem C, Heyndrickx GR, De Bruyne B, Wijns W. Revascularization decisions in patients with stable angina and intermediate lesions: results of the international survey on interventional strategy. *Circ Cardiovasc Interv*. 2014;7:751–759.
- Douglas PS, Pontone G, Hlatky MA, Patel MR, Norgaard BL, Byrne RA, Curzen N, Purcell I, Gutberlet M, Rioufol G, Hink U, Schuchlenz HW, Feuchtnr G, Gilard M, Andreini D, Jensen JM, Hadamitzky M, Chiswell K, Cyr D, Wilk A, Wang F, Rogers C, De Bruyne B; PLATFORM Investigators. Clinical outcomes of fractional flow reserve by computed tomographic angiography-guided diagnostic strategies vs. Usual care in patients with suspected coronary artery disease: the prospective longitudinal trial of FFR(CT): outcome and resource impacts study. *Eur Heart J*. 2015;36:3359–3367.
- Morris PD, Ryan D, Morton AC, Lycett R, Lawford PV, Hose DR, Gunn JP. Virtual fractional flow reserve from coronary angiography: modeling the significance of coronary lesions: results from the VIRTU-1 (VIRTUal Fractional Flow Reserve From Coronary Angiography) study. *JACC Cardiovasc Interv*. 2013;6:149–157.
- Papafaklis MI, Muramatsu T, Ishibashi Y, Lakkas LS, Nakatani S, Bourantas CV, Ligthart J, Onuma Y, Echavarría-Pinto M, Tzirka G, Kotsia A, Nikas DN, Mogabgab O, van Geuns RJ, Naka KK, Fotiadis DI, Brilakis ES, Garcia-Garcia HM, Escaned J, Zijlstra F, Michalis LK, Serruys PW. Fast virtual functional assessment of intermediate coronary lesions using routine angiographic data and blood flow simulation in humans: comparison with pressure wire—fractional flow reserve. *EuroIntervention*. 2014;10:574–583.
- Kornowski R, Lavi I, Pellicano M, Xaplanteris P, Vaknin-Assa H, Assali A, Valtzer O, Lotringer Y, De Bruyne B. Fractional flow reserve derived from routine coronary angiograms. *J Am Coll Cardiol*. 2016;68:2235–2237.
- Norgaard BL, Leipsic J, Gaur S, Seneviratne S, Ko BS, Ito H, Jensen JM, Mauri L, De Bruyne B, Bezerra H, Osawa K, Marwan M, Naber C, Erglis A, Park SJ, Christiansen EH, Kalltoft A, Lassen JF, Botker HE, Achenbach S; NXT Trial Study Group. Diagnostic performance of noninvasive fractional flow reserve derived from

- coronary computed tomography angiography in suspected coronary artery disease: the NXT trial (Analysis of Coronary Blood Flow Using CT Angiography: Next Steps). *J Am Coll Cardiol*. 2014;63:1145–1155.
9. Koo BK, Erglis A, Doh JH, Daniels DV, Jegere S, Kim HS, Dunning A, DeFrance T, Lansky A, Leipsic J, Min JK. Diagnosis of ischemia-causing coronary stenoses by noninvasive fractional flow reserve computed from coronary computed tomographic angiograms. Results from the prospective multicenter discover-flow (diagnosis of ischemia-causing stenoses obtained via noninvasive fractional flow reserve) study. *J Am Coll Cardiol*. 2011;58:1989–1997.
 10. Min JK, Leipsic J, Pencina MJ, Berman DS, Koo BK, van Mieghem C, Erglis A, Lin FY, Dunning AM, Apruzzese P, Budoff MJ, Cole JH, Jaffer FA, Leon MB, Malpeso J, Mancini GB, Park SJ, Schwartz RS, Shaw LJ, Mauri L. Diagnostic accuracy of fractional flow reserve from anatomic CT angiography. *JAMA*. 2012;308:1237–1245.
 11. Tu S, Westra J, Yang J, vonBergelen C, Ferrara A, Pellicano M, Nef H, Tebaldi M, Murasato Y, Lansky A, Barbato E, van der Heijden LC, Reiber JH, Holm NR, Wijns W; FAVOR Pilot Trial Study Group. Diagnostic accuracy of fast computational approaches to derive fractional flow reserve from diagnostic coronary angiography: the international multicenter FAVOR pilot study. *JACC Cardiovasc Interv*. 2016;9:2024–2035.
 12. Xu B, Tu S, Qiao S, Qu X, Chen Y, Yang J, Guo L, Sun Z, Li Z, Tian F, Fang W, Chen J, Li W, Guan C, Holm NR, Wijns W, Hu S. Diagnostic accuracy of angiography-based quantitative flow ratio measurements for online assessment of coronary stenosis. *J Am Coll Cardiol*. 2017;70:3077–3087.
 13. Abaci A, Oguzhan A, Eryol NK, Ergin A. Effect of potential confounding factors on the thrombolysis in myocardial infarction (TIMI) trial frame count and its reproducibility. *Circulation*. 1999;100:2219–2223.
 14. Toth GG, Johnson NP, Jeremias A, Pellicano M, Vranckx P, Fearon WF, Barbato E, Kern MJ, Pijls NH, De Bruyne B. Standardization of fractional flow reserve measurements. *J Am Coll Cardiol*. 2016;68:742–753.
 15. Westra J, Tu S, Winther S, Nissen L, Vestergaard MB, Andersen BK, Holck EN, Fox Maule C, Johansen JK, Andreasen LN, Simonsen JK, Zhang Y, Kristensen SD, Maeng M, Kalltoft A, Terkelsen CJ, Krusell LR, Jakobsen L, Reiber JHC, Lassen JF, Bottocher M, Botker HE, Christiansen EH, Holm NR. Evaluation of coronary artery stenosis by quantitative flow ratio during invasive coronary angiography: the WIFI II Study (Wire-Free Functional Imaging II). *Circ Cardiovasc Imaging*. 2018;11:e007107.
 16. Pellicano M, Lavi I, De Bruyne B, Vakin-Assa H, Assali A, Valtzer O, Lotringer Y, Weisz G, Almagor Y, Xaplanteris P, Kirtane AJ, Codner P, Leon MB, Kornowski R. Validation study of image-based fractional flow reserve during coronary angiography. *Circ Cardiovasc Interv*. 2017;10:e005259.
 17. Morris PD, Silva Soto DA, Feher JFA, Rafiroiu D, Lungu A, Varma S, Lawford PV, Hose DR, Gunn JP. Fast virtual fractional flow reserve based upon steady-state computational fluid dynamics analysis: results from the VIRTU-Fast study. *JACC Basic Transl Sci*. 2017;2:434–446.
 18. Fihn SD, Gardin JM, Abrams J, Berra K, Blankenship JC, Dallas AP, Douglas PS, Foody JM, Gerber TC, Hinderliter AL, King SB III, Kligfield PD, Krumholz HM, Kwong RY, Lim MJ, Linderbaum JA, Mack MJ, Munger MA, Prager RL, Sabik JF, Shaw LJ, Sikkema JD, Smith CR Jr, Smith SC Jr, Spertus JA, Williams SV; American College of Cardiology Foundation, American Heart Association Task Force on Practice Guidelines, American College of Physicians, American Association for Thoracic Surgery, Preventive Cardiovascular Nurses Association, Society for Cardiovascular Angiography and Interventions, Society of Thoracic Surgeons. 2012 ACCF/AHA/ACP/AATS/PCNA/SCAI/STS Guideline for the diagnosis and management of patients with stable ischemic heart disease: a report of the American College of Cardiology Foundation/American Heart Association Task Force on Practice Guidelines, and the American College of Physicians, American Association for Thoracic Surgery, Preventive Cardiovascular Nurses Association, Society for Cardiovascular Angiography and Interventions, and Society of Thoracic Surgeons. *J Am Coll Cardiol*. 2012;60:e44–e164.
 19. Dattilo PB, Prasad A, Honeycutt E, Wang TY, Messenger JC. Contemporary patterns of fractional flow reserve and intravascular ultrasound use among patients undergoing percutaneous coronary intervention in the United States: insights from the national cardiovascular data registry. *J Am Coll Cardiol*. 2012;60:2337–2339.
 20. Jeremias A, Maehara A, Genereux P, Asrress KN, Berry C, De Bruyne B, Davies JE, Escaned J, Fearon WF, Gould KL, Johnson NP, Kirtane AJ, Koo BK, Marques KM, Nijjer S, Oldroyd KG, Petraco R, Piek JJ, Pijls NH, Redwood S, Siebes M, Spaan JA, van't Veer M, Mintz GS, Stone GW. Multicenter core laboratory comparison of the instantaneous wave-free ratio and resting PD/PA with fractional flow reserve: the RESOLVE study. *J Am Coll Cardiol*. 2014;63:1253–1261.
 21. Petraco R, van de Hoef TP, Nijjer S, Sen S, van Lavieren MA, Foale RA, Meuwissen M, Broyd C, Echavarría-Pinto M, Foin N, Malik IS, Mikhail GW, Hughes AD, Francis DP, Mayet J, Di Mario C, Escaned J, Piek JJ, Davies JE. Baseline instantaneous wave-free ratio as a pressure-only estimation of underlying coronary flow reserve: results of the JUSTIFY-CFR study (Joined Coronary Pressure and Flow Analysis to Determine Diagnostic Characteristics of Basal and Hyperemic Indices of Functional Lesion Severity-Coronary Flow Reserve). *Circ Cardiovasc Interv*. 2014;7:492–502.
 22. Petraco R, Park JJ, Sen S, Nijjer SS, Malik IS, Echavarría-Pinto M, Asrress KN, Nam CW, Macias E, Foale RA, Sethi A, Mikhail GW, Kaprielian R, Baker CS, Lefroy D, Bellamy M, Al-Bustami M, Khan MA, Gonzalo N, Hughes AD, Francis DP, Mayet J, Di Mario C, Redwood S, Escaned J, Koo BK, Davies JE. Hybrid iFR-FFR decision-making strategy: implications for enhancing universal adoption of physiology-guided coronary revascularisation. *EuroIntervention*. 2013;8:1157–1165.
 23. Gotberg M, Christiansen EH, Gudmundsdottir IJ, Sandhall L, Danielewicz M, Jakobsen L, Olsson SE, Ohagen P, Olsson H, Omerovic E, Calais F, Lindroos P, Maeng M, Todt T, Venetsanos D, James SK, Kareglen A, Nilsson M, Carlsson J, Hauer D, Jensen J, Karlsson AC, Panayi G, Erlinge D, Frobert O. Instantaneous wave-free ratio versus fractional flow reserve to guide pci. *N Engl J Med*. 2017;376:1813–1823.
 24. Davies JE, Sen S, Dehbi HM, Al-Lamee R, Petraco R, Nijjer SS, Bhandi R, Lehman SJ, Walters D, Sapontis J, Janssens L, Vrints CJ, Khashaba A, Laine M, Van Belle E, Krackhardt F, Bojara W, Going O, Harle T, Indolfi C, Niccoli G, Ribichini F, Tanaka N, Yokoi H, Takashima H, Kikuta Y, Erglis A, Vinhas H, Canas Silva P, Baptista SB, Alghamdi A, Hellig F, Koo BK, Nam CW, Shin ES, Doh JH, Brugaletta S, Alegria-Barrero E, Meuwissen M, Piek JJ, van Royen N, Sezer M, Di Mario C, Gerber RT, Malik IS, Sharp AS, Talwar S, Tang K, Samady H, Altman J, Seto AH, Singh J, Jeremias A, Matsuo H, Kharbada RK, Patel MR, Serruys P, Escaned J. Use of the instantaneous wave-free ratio or fractional flow reserve in PCI. *N Engl J Med*. 2017;376:1824–1834.
 25. Johnson NP, Toth GG, Lai D, Zhu H, Acar G, Agostoni P, Appelman Y, Arslan F, Barbato E, Chen SL, Di Serafino L, Dominguez-Franco AJ, Dupouy P, Esen AM, Esen OB, Hamilos M, Iwasaki K, Jensen LO, Jimenez-Navarro MF, Katritsis DG, Kocaman SA, Koo BK, Lopez-Palop R, Lorin JD, Miller LH, Muller O, Nam CW, Oud N, Puymirat E, Rieber J, Rioufol G, Rodes-Cabau J, Sedlis SP, Takeishi Y, Tonino PA, Van Belle E, Verna E, Werner GS, Fearon WF, Pijls NH, De Bruyne B, Gould KL. Prognostic value of fractional flow reserve: linking physiologic severity to clinical outcomes. *J Am Coll Cardiol*. 2014;64:1641–1654.
 26. Spitaleri G, Tebaldi M, Biscaglia S, Westra J, Brugaletta S, Erriquez A, Passarini G, Brieda A, Leone AM, Picchi A, Ielasi A, Girolamo DD, Trani C, Ferrari R, Reiber JHC, Valgimigli M, Sabate M, Campo G. Quantitative flow ratio identifies nonculprit coronary lesions requiring revascularization in patients with ST-segment-elevation myocardial infarction and multivessel disease. *Circ Cardiovasc Interv*. 2018;11:e006023.

SUPPLEMENTAL MATERIAL

Data S1.

Supplemental Methods

Sample size calculation

Estimates for the sample size calculation were based on the results from the FAVOR study, where a sensitivity of 0.74 and a specificity of 0.91 for QFR were found. The null hypothesis was H_0 : Sensitivity(QFR \leq 0.80) = Sensitivity(%DS \leq 50) and H_1 : Unequal sensitivities for the two methods. A normal-approximate McNemar test with the Connor method was performed; Proportion1=0.48; proportion2=0.74; correlation=-0.1. We did similar for specificity (H_0 : Specificity(QFR $>$ 0.80) = Specificity(DS $>$ 50), and H_1 : Unequal specificities for the two methods; Proportion1=0.75; proportion2=0.91; correlation=0.4. With power=0.90, alpha=0.05 and a rate of true positives in the population of estimated 30%, a total of 274 patients with paired QFR and FFR were required to reject the null hypothesis for sensitivity and 257 for specificity. To accommodate for insufficient angiographic quality or failed FFR a total of 310 patients were estimated to be required.

Secondary endpoints

Feasibility

The feasibility was assessed as the fraction of lesions with successful FFR measurements where QFR was computed.

Time to QFR and FFR

Time to QFR was defined as start of frame selection for the three-dimensional reconstruction of the vessel until QFR was computed using contrast flow evaluation. Time to FFR was defined as the

introduction of the pressure wire to the guiding catheter until drift check with a drift value within the specified limits.

QFR/FFR hybrid-approach limits

For a QFR/FFR hybrid strategy we used an FFR-only strategy as gold standard. QFR limits to yield a sensitivity (QFR-treat) and specificity (QFR-defer) of 90 and 95 percent were identified and used to model a hybrid approach where wire-based FFR assesment is needed between the QFR-treat and QFR-defer limits. The proportion of potential pressure wire free lesion assessments was calculated.

Prediction of QFR-FFR discrepancy

We constructed a multilevel mixed effect model including sites as level variable. Following co-variates were tested individually and included in the multivariate analysis if $P\text{-value} < 0.10$: lesion length, % DS (2D-QCA), age, BMI, adenosine route, sex, smoking, vessel, diabetes, previous PCI, and FFR.

Procedure training

Participating sites were requested to have operators and dedicated staff trained on QFR computation. The staff received instructions and training from Medis medical imaging bv. Only staff with QFR certificates obtained from Medis could perform the study computation of QFR. Besides the QFR training from Medis, all sites were required to submit at least two complete and fully anonymized training datasets for approval by the respective core-labs before study enrolment.

Site specific blinding protocol

Blinding was ensured by one of the following site-specific strategies: 1) QFR was computed simultaneously in a separate room (Skejby, Naples, Ferrara, Warsaw, Gifu, Madrid, Essen, Mestre)
2) QFR was performed before FFR (Caserta, Skejby, Hague).

Data S2.

FAVOR II standard operating procedure for QFR computation in FAVOR II Europe-Japan

The QFR standard operating procedure (SOP) applied by all sites in the FAVOR II multicenter study by Aarhus University Hospital, Skejby, Denmark. The set of instructions do not constitute a manual, neither partly nor in full, for clinical use of QFR.

1. Identification of cases not appropriate for QFR during coronary angiography (angiographic exclusion criteria)

1.1 Aorto-ostial stenosis

Aorto-ostial stenosis is not analyzable by QFR at present due to the requirement of two optimal projections, the guiding catheter intrusion and back flow of contrast in aorta overlapping the ostium.

1.2 Low angiographic quality or poor contrast filling

In some cases, the application is not able to recognize the vessel contours due to excessively low angiographic quality or poor contrast filling and exclusion of the case can be necessary (fig. 1).

With experience the operator may decide to exclude the case even before transmitting runs to the QFR work station for analysis.

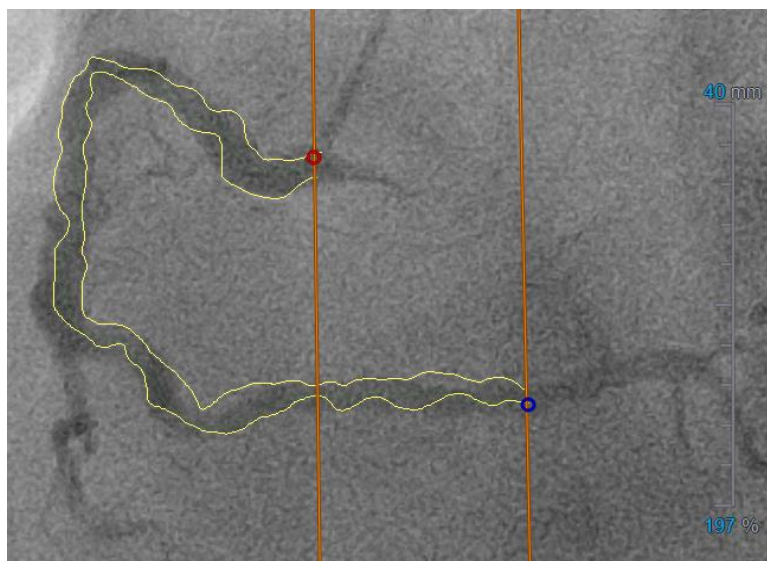


Figure 1 Low angiographic quality. The QFR application has difficulties finding the vessel lumen and vessel borders.

1.3 **Overlap**

If correct lumen contouring is impossible due to severe overlap of the stenosed segment, the case should be excluded.

1.4 **Nitroglycerin administration**

When nitroglycerin is not administered neither systemic nor intracoronary, vessel spasms cannot be ruled out, and the case should be excluded (fig. 2). Without prior nitroglycerin, both the QFR analysis and FFR measurement can be unreliable.

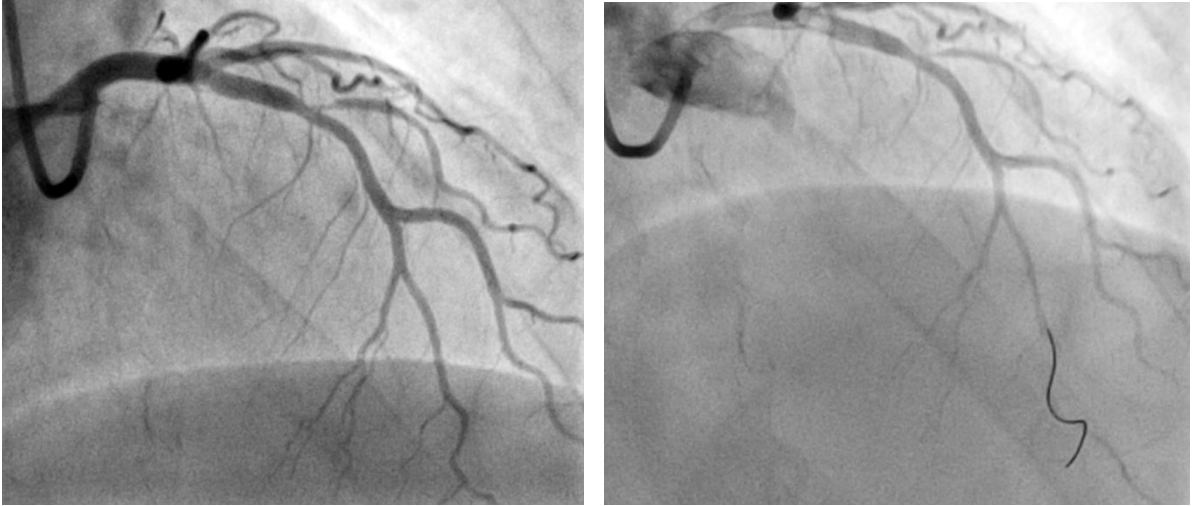


Figure 2 FFR measurement without nitroglycerin before and after advancement of wire. The wire causes the vessel to spasm and therefore the FFR value is unreliable.

1.5 **Stenosis at or near large diameter shifts**

QFR validity is unknown in bifurcation lesions if the stenosis involves both sides of a major shift (>1 mm) in reference diameter. This includes:

- Patients with lesions in the distal LMCA and the ostium of the Cx.

1.6 **Severe tortuosity of target vessel**

Severely tortuous vessels where excess foreshortening of the stenosed segments cannot avoided should not be analyzed by QFR.

2. Step-by-step manual

The Medis Suite QAngio XA 3D/QFR solution (Medis medical imaging system bv, Leiden, The Netherlands) is used for computation of QFR in FAVOR II. The Medis Suite QAngio XA 3D/QFR solution requires installation on a Windows-based computer. QFR computation is described step-by-step below.

2.1 Coronary angiography

Two good projections at least 25 degrees apart are required for the 3D vessel reconstruction.

Angiographic procedure:

- Inject I.C. nitroglycerin as early as possible
- Use framerate of at least 12.5 frames/sec
- Make sure that the catheter is filled with contrast before the injection (i.e. after administration of nitroglycerin)
- Use brisk, continuous and fast contrast injections. Aim for filling during full 3 cardiac cycles
- Minimize overlap of target segments
- Avoid foreshortening of the vessel
- Avoid zooming but use of other means to increase image quality are encouraged.
- Avoid moving the table early after injection
- Aim for projections perpendicular to the target vessel – consider suggested projections (table1)
- Make sure that the entire vessel is visible in both projections. Both the guiding catheter tip and the potential position of the FFR pressure transducer should be visible in the same frame

Suggested projections are found in table 1.

Table 1 Recommended projection angles for specific lesion segments. Angulation of more than 25° between projections is required.

Vessel /Bifurcation	1st View	2nd View
LM + LAD/LCX	RAO 20, Caudal 45	AP, Caudal 10
LAD/Diag	AP, Cranial 45	RAO 35, Cranial 20
LCX/OM	LAO 10, Caudal 25	RAO 25, Caudal 25
Proximal+Mid RCA	LAO 45, CAUD 0	AP, CAUD 0
PLA/PDA	LAO 45, CAUD 0	LAO 30, CAUD 30

If only one good projection is identified, consider to use the *Acquisition Guide* in the Medis Suite

QAngio XA 3D/QFR solution to identify the second projection:

1. Transfer first good projection to QFR computer (see 2.2)
2. Right-click on the projection and start the QAngio XA 3D application
3. Choose *Acquisition Guide* (fig.3, red box). The yellow line indicates the new projection angle, and should be approximately perpendicular to the target vessel at the lesion site

- a. If several lesions are located in the same vessel, a compromise must be made to ensure that most of the lesions and the most severe lesions are seen in the same projection
4. Move the projection line by moving the yellow spot (fig.3, white arrow) in the Acquisition Guide indicator. Aim to keep the yellow spot inside the green area and to achieve an angle difference of 30-50 degrees
5. Position the C-arm as proposed by the guide
6. In case of excessive overlap of the target segments and other vessels, rotate the C-arm 5 degrees around the axis of the target vessel
 - a. If needed, use the Acquisition guide indicator again by maintaining the angulation of the yellow line and move the yellow spot just outside the green area – away from the red area. Move the C-arm accordingly to the new proposition

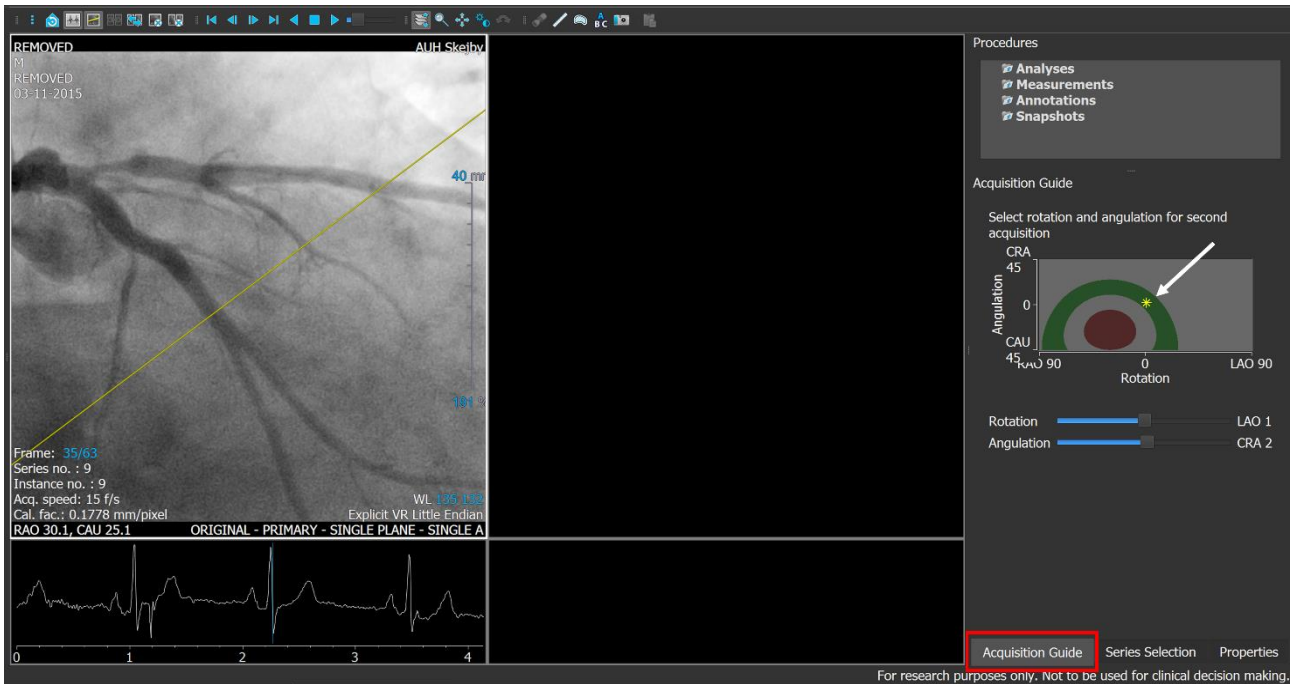


Figure 3 Acquisition projection angle. Red box: Acquisition guide. White arrow: Yellow spot indicating position of C-arm.

2.2 Image transfer

The angiographic runs are transferred to the QFR-computer using an angiographic equipment specific protocol.

2.3 Angiographic run selection

Optimal projections are chosen according to the following criteria:

- Minimal overlap of the target vessel
- Good contrast injection, filling the entire vessel
- Includes both the healthy part of the vessel proximal to the first stenosis and the location of the pressure transducer of the subsequent FFR assessment

Workflow in angiographic run selection

1. Identify the optimal projection and right-click the best run. Start QAngio XA 3D
2. Choose *Series Selection* (fig.4, red box) to get a presentation of angiographic runs that are ≥ 25 degrees different from the selected run
3. Evaluate the potential runs by dragging them into the empty, right panel
 - If the two projections are not 25 degrees apart, you can change the minimum angle in the pop-up menu in Options. It is not recommended to do the 3D reconstruction based on runs <25 degrees apart
4. Keep the best 2nd run in the panel with the epipolar line perpendicular to the lesion(s)

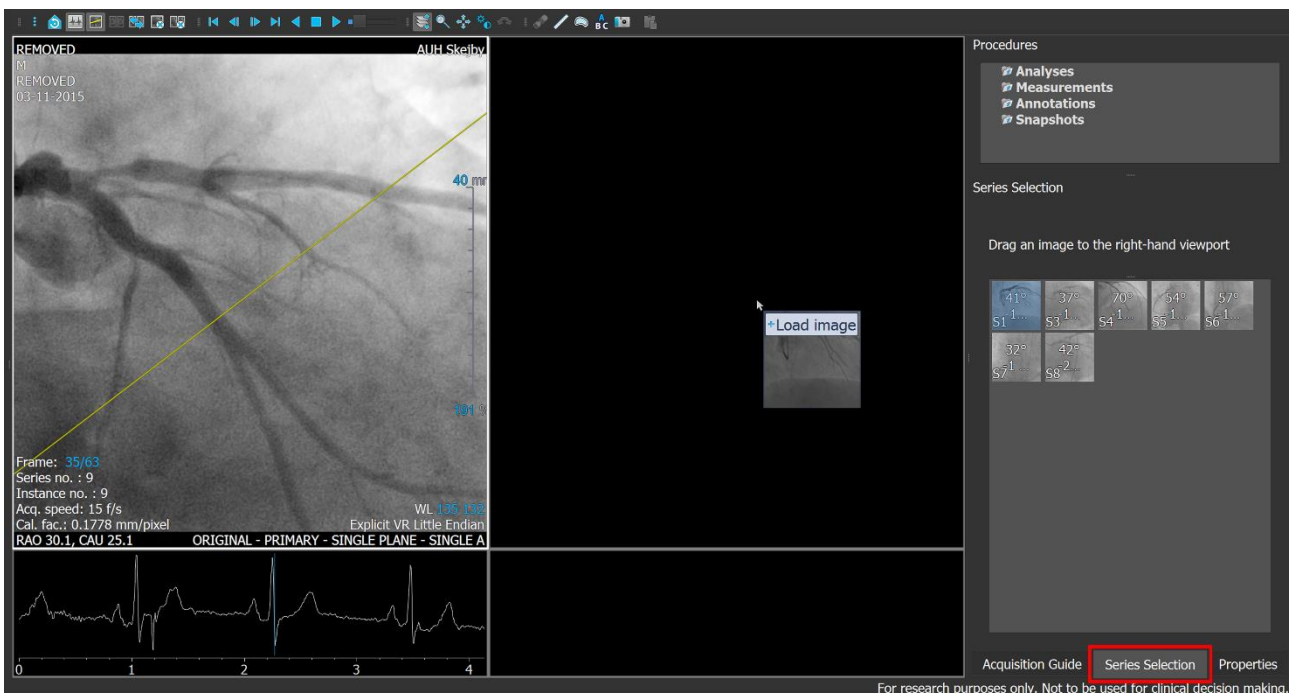


Figure 4 Angiographic run selection. Red box: Series Selection.

2.4 Frame selection

The best frames for analysis are selected by ensuring:

- The lesion site(s) is not overlapped
- The entire vessel is filled with contrast
- Frame includes both the healthy part of the vessel proximal to the first stenosis and the location of the pressure transducer of the subsequent FFR assessment
- Frames are "end-diastolic" – preferably frames recorded between the P-wave and the QRS-complex (fig.5)

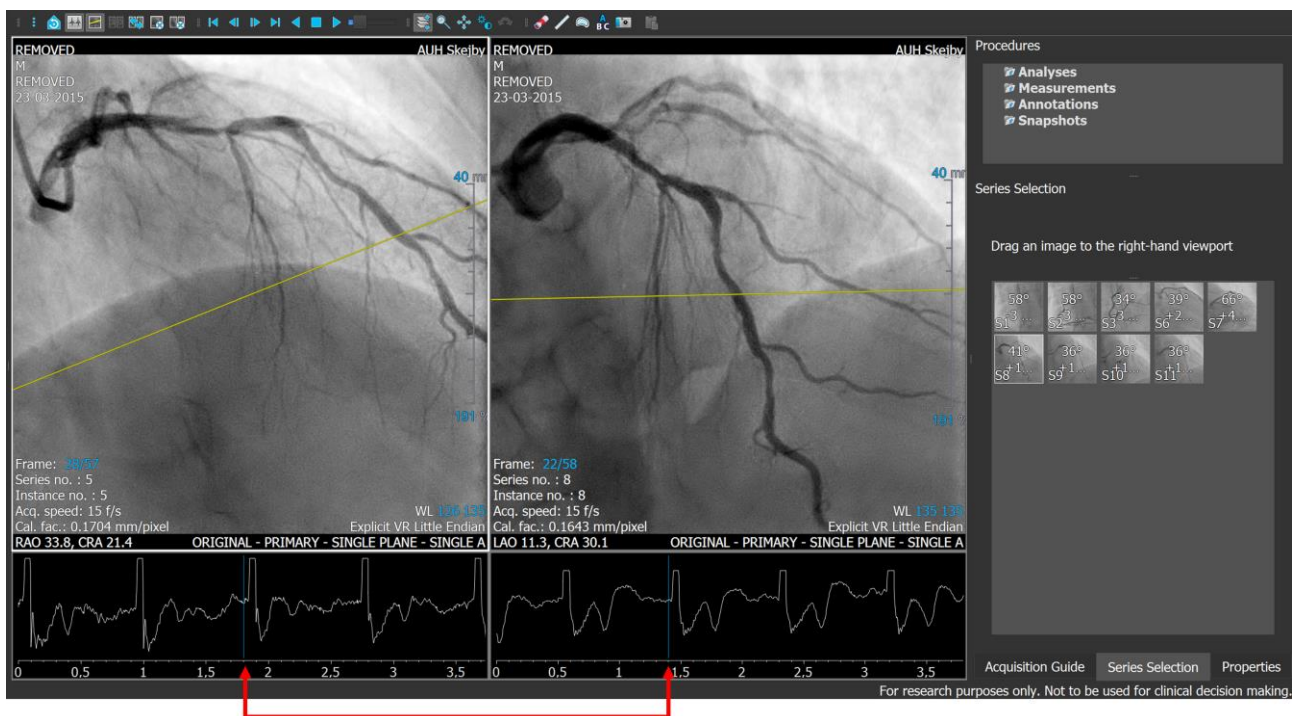


Figure 5 Frame selection. Note that both runs are in the same end-diastolic phase and the epipolar line is perpendicular to the lesions.

When the best end diastolic frame is found in both panels, the 3D reconstruction is initiated by pressing the *Create single vessel analysis*-button (fig. 6, red arrow) in the top panel.

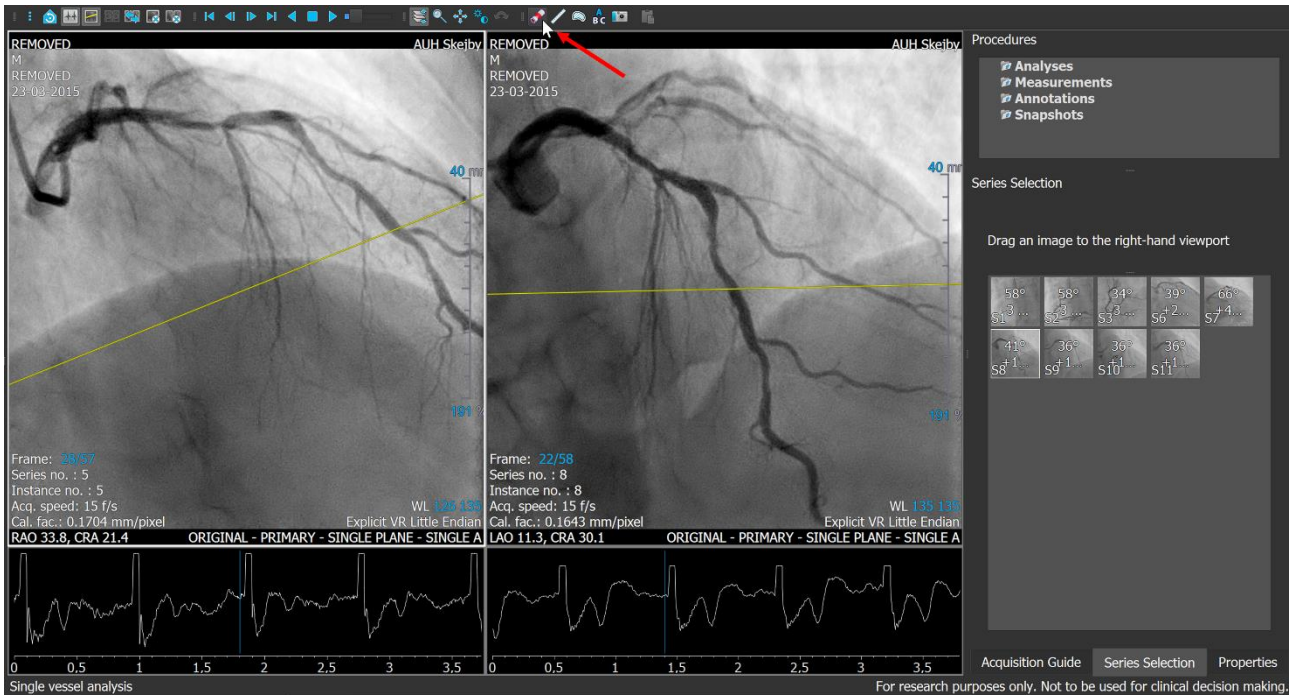


Figure 6 Create single vessel analysis (marked by red arrow) initiates the 3D reconstruction.

2.5 3D target vessel reconstruction

To link the two projections, corresponding landmarks near the lesion are identified by a pair of offset points in both projections (fig. 7). Make sure to:

- Identify a landmark that is easily identified in both projections (i.e. a bifurcation, a localized stenosis or the off-spring of a side branch)
- If using a side branch:
 - Select a side branch that departs perpendicularly from the main branch - if possible
 - Place the offset point in the middle of the main vessel

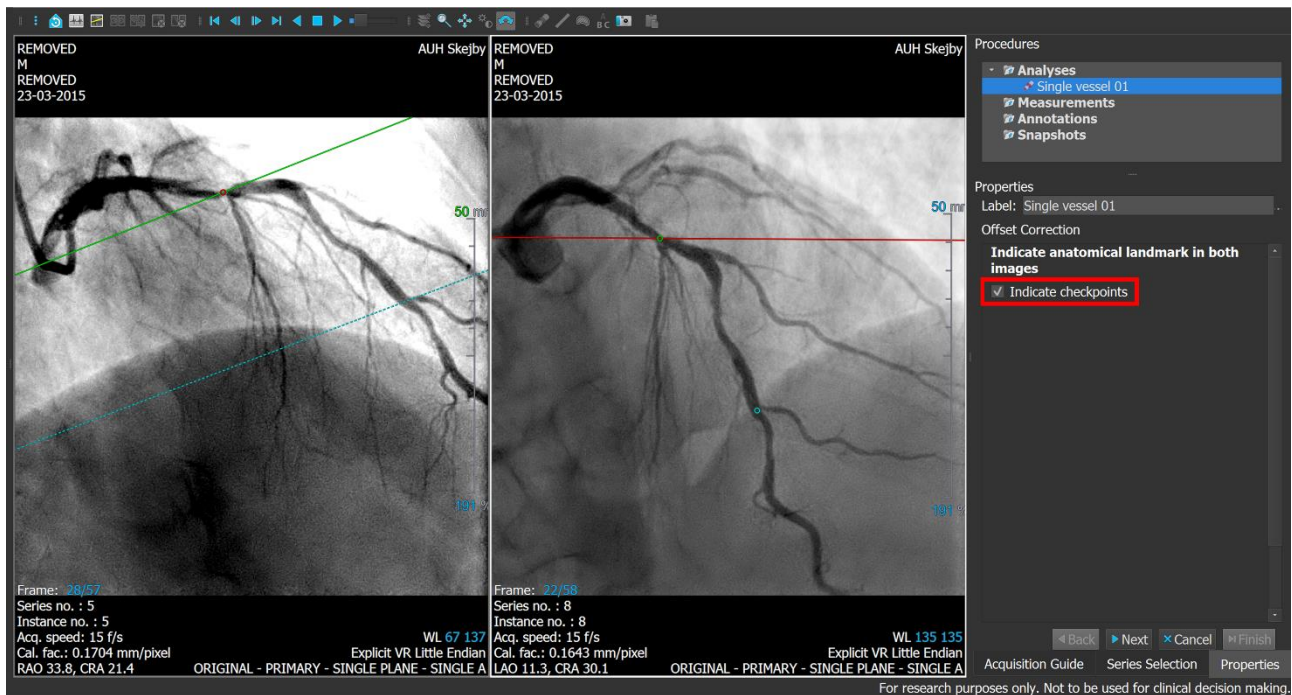


Figure 7 Corresponding point is marked by the red and green spot in the left and right panel, respectively. In this example, the offspring of a side branch/lesion point is easily recognized in both projections, is selected as the point to correspond.

- Use the *Indicate checkpoints* option, to make sure that the projections are linked together properly.
 - Tick off the *Indicate checkpoints* box (fig. 7, red box)
 - Choose another landmark, identifiable in both projections (i.e. a bifurcation, a stenosis or the off-spring of a side branch)
 - Put a checkpoint proximal and distal to the corresponding point or place another checkpoint to check the agreement for reconstruction between the two projections

The matching checkpoints are shown as a circle in one projection and as a dotted line in the other, in the same colour.

- Revise the position of the chosen offset point or select an entirely different location for the offset point if the checkpoints are not consistent in the two projections

2.6 Indicating target vessel

Indication of the boarder of segment to analyse

- 1) Ensure that the analysed segment includes reference segments at both ends for optimal reference vessel reconstruction
- 2) The proximal path line point is placed in a “most healthy” part of the vessel, proximal to all stenotic segments
- 3) When the proximal path line point is added in one panel, a corresponding support line is shown in the other panel. The proximal path line point in the second projection is placed on this support line at the same anatomical location
 - a. If the corresponding support line is parallel to the proximal or distal part of the vessel it can be necessary to place the proximal point in relation to an anatomical landmark that can be recognized in both projections
 - b. If the proximal parts of the vessel corresponds poorly, the proximal point in the second projection should not be placed at the indicator line, but landmarks should be used to ensure the same position of the proximal points in the two projections-
Later, the projections may need to be “*forced corresponded*” (see 2.9).
- 4) The distal point is placed at least as far down as the pressure transducer is positioned during the FFR measurement

After indicating proximal and distal points in both projections, the vessel pathline (fig. 8) is shown.

The path line is verified visually for both projections. If it deviates from the target vessel, it is dragged into position using support points.

When the position of the vessel pathline is accepted, the pathline is “locked” (fig. 8, red box).

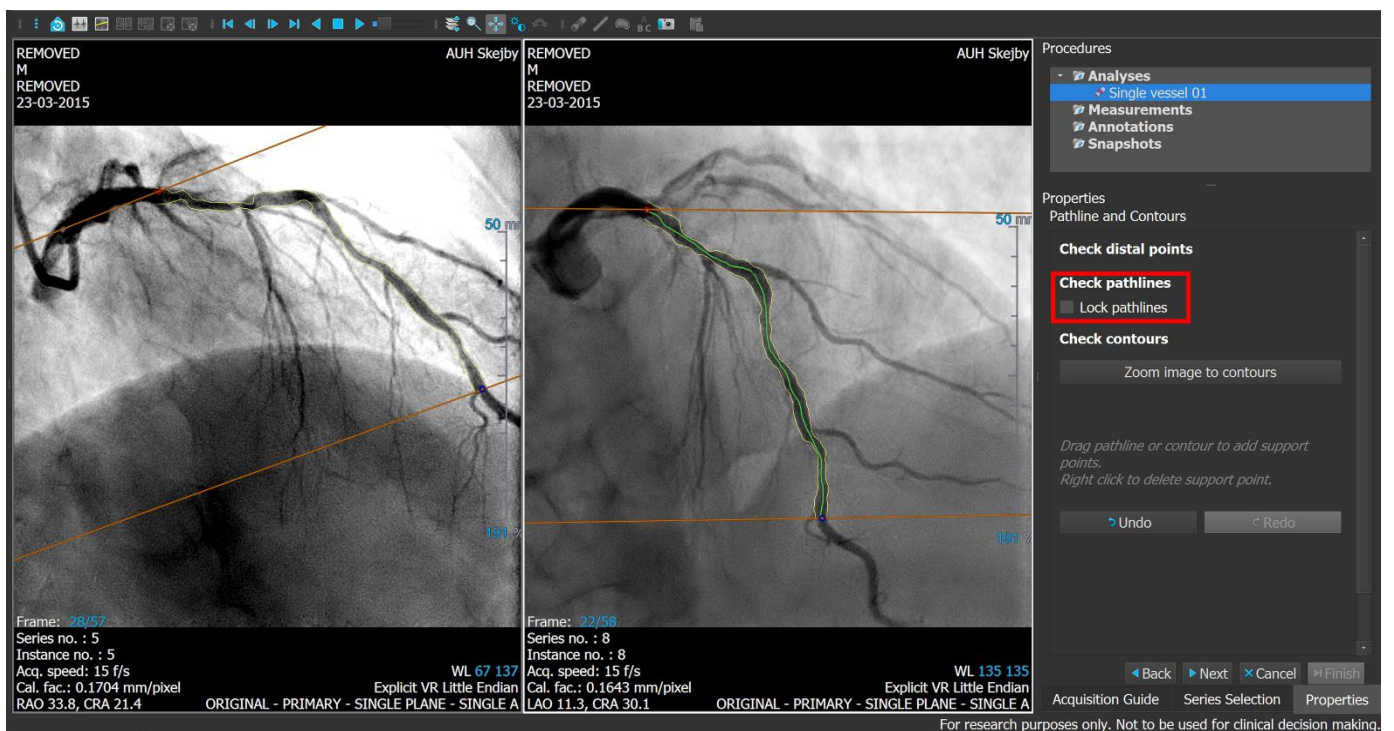


Figure 8 Segmented target vessel. The proximal point is marked by red circles while the distal point is marked by blue circles. The target vessel pathline is indicated by the green line in the right panel. It is visible when the mouse is shifted over it. The pathline is fixated by ticking Lock pathlines (red box).

2.7 Lumen contouring

The yellow contour lines (fig. 9) are adjusted to follow the lumen border. **Pay special attention to:**

- Indication of non-existing narrowings in the proximal and distal ends
- Correct contouring of the target lesion(s)
- Side branches and overlap
- Ensure that contours are correct in all segments – also non-target segments as it influences QFR calculation

The lines are corrected by dragging them into position with correction points. If a correction needs to be reverted, right-click the created correction-point and it will be deleted.

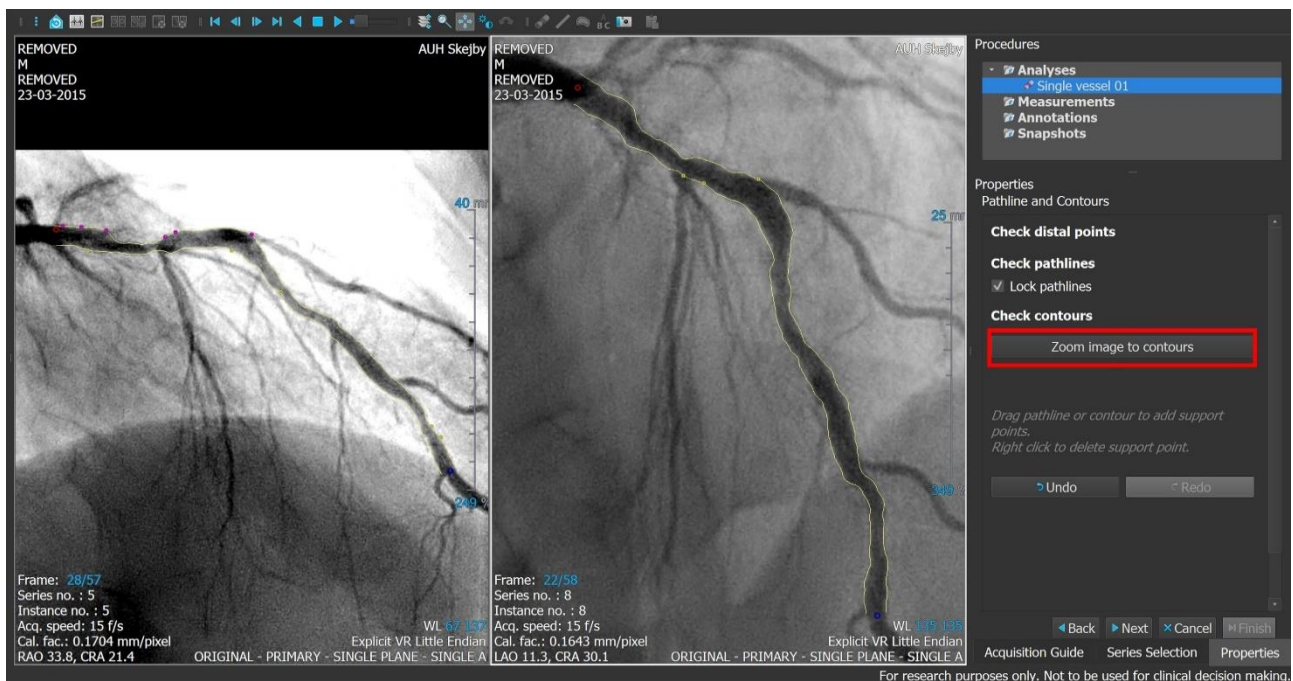


Figure 9 Lumen contouring. The yellow lines indicate the lumen border, and can be corrected by dragging them into position (note the placed correction points). To get a better view, click “zoom image to contours (red box).

2.8 Forced correspondence

Correspondence is automatically performed, but manual forced corresponding points can be added for editing. With this tool, the two centerlines are forced to correspond at an indicated point. Forced correspondence is particularly important when the graphs for the two minimal and maximal diameters in lower right panel are shifted sideways instead of being almost superimposed (fig. 10).

- 1) Identify an anatomical landmark easily identified in both projections (i.e. the narrowest part of the target lesion or the off-spring of a side branch)

Tick Corresponding points

- 1) Indicate the landmark in both projections
- 2) Check if the curves of maximum and minimum diameters are now more aligned
- 3) Adjust the markers until finding the best possible correspondence, with good alignment of the two curves

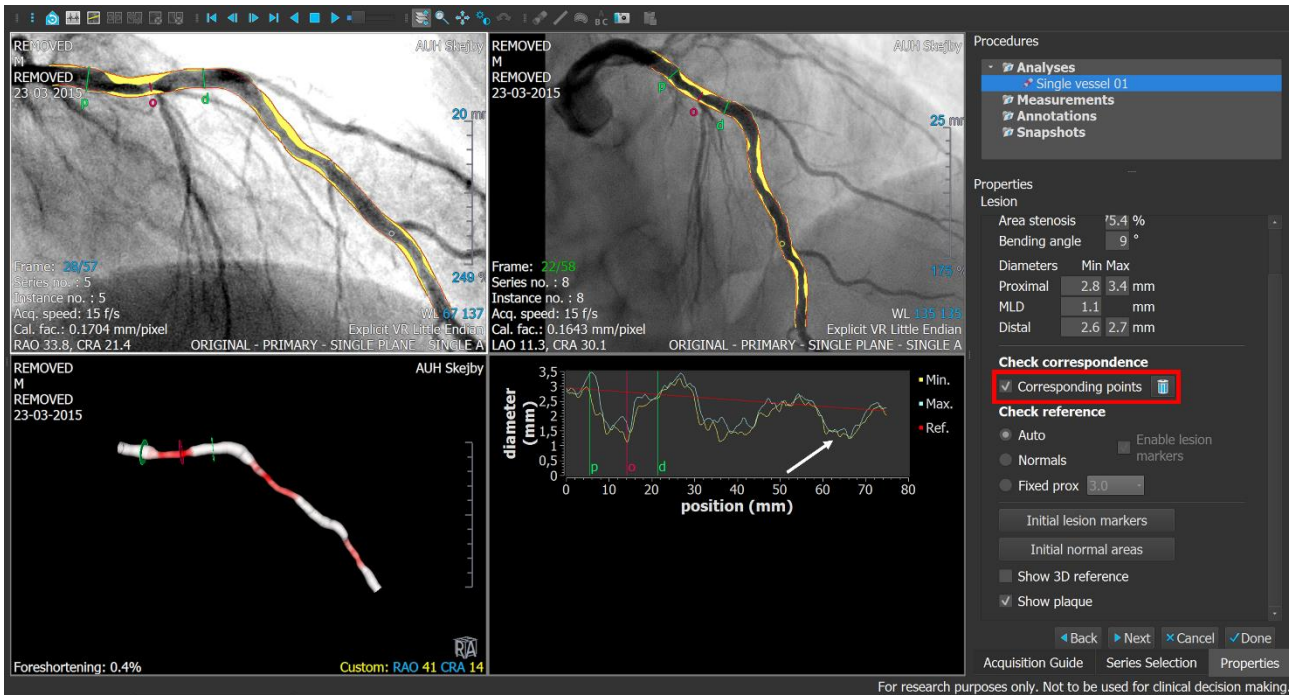


Figure 10 Forced corresponding points. The option is marked (red box) and landmarks are selected (see text). Note the improved distal alignment between the two diameter functions (blue and yellow lines. White arrow) compared to figure 10-12.

NOTE: Focus on getting the lesions and proximal vessel segments to correspond. Use the lesion markers to check the correspondence at this step before proceeding.

2.9 Reference vessel

Every part of the contoured lumen that is narrower than the reference vessel is marked yellow as plaque (fig. 11). These yellow markings can be removed by ticking off the box *Show plaque* (Figure 11, red box).

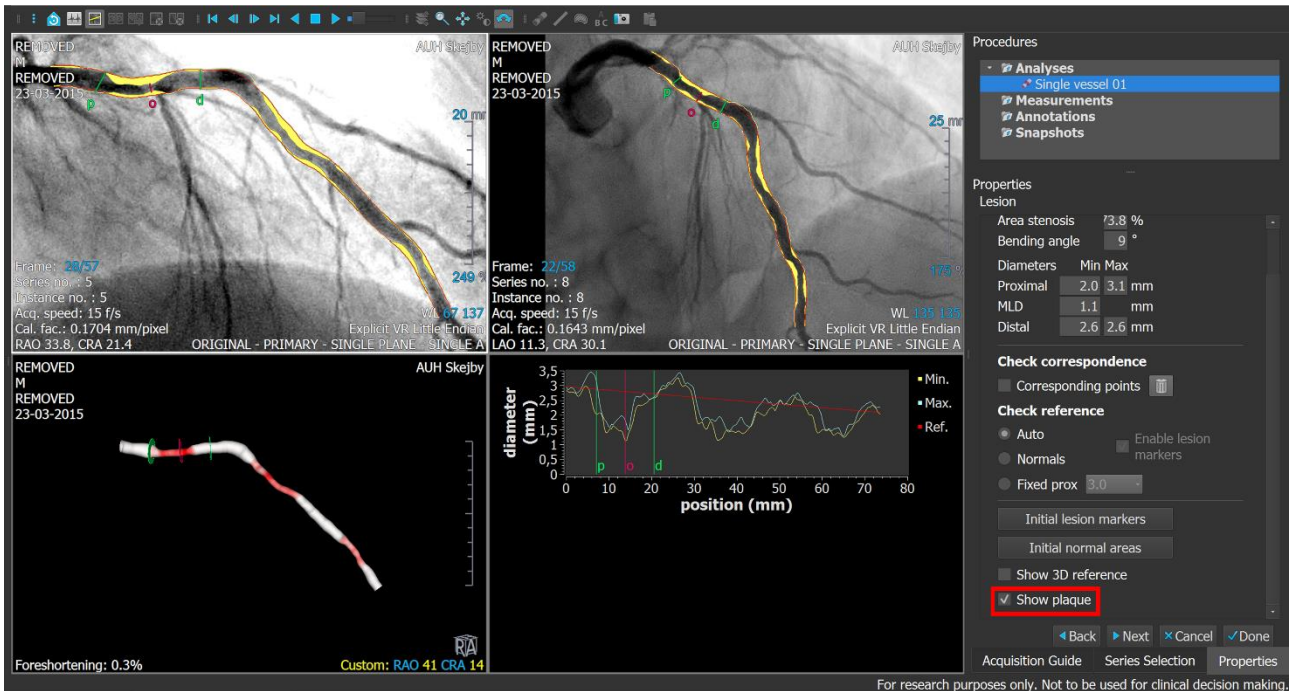


Figure 11 Reference vessel (red contours on 2D images). Show/hide yellow plaque (red box).

The proximal and distal ends are supposed to approximately match the healthy vessel parts. The reference function should obey the following:

- Always tapering reference function. A straight function is allowed in short segments.
- Should not follow stenosed or aneurysmatic sections.
- Sizes should be realistic according to gender and body mass index. See 2.9.3

If the abovementioned criteria are not fulfilled, the reference contours can be edited as follows:

2.9.1 Selection of normal areas

Select “Normals” under the “check reference wizard” (text fig. 12, red box). Select two normal areas, using the green areas. The reference function is now calculated as a linear regression based on the two selected normals. Note the slightly adjusted reference contours after using the “Normals” function (fig. 12 compared to fig. 11).

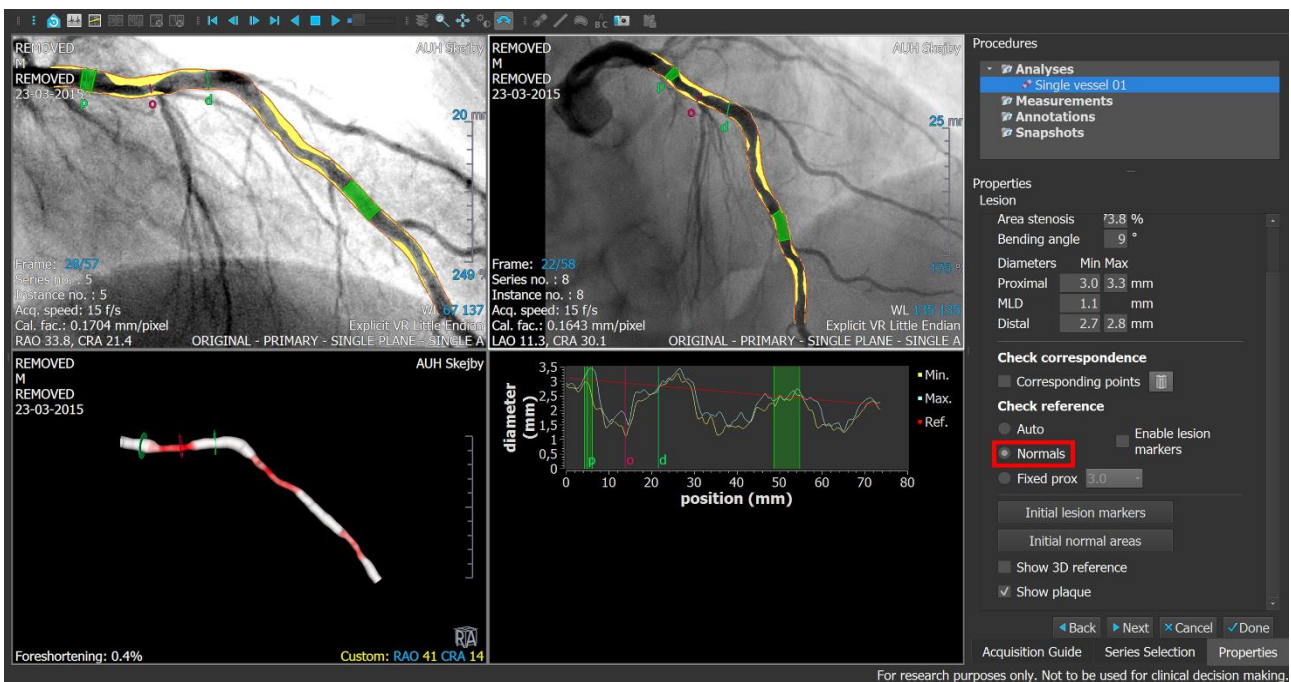


Figure 12 Reference function editing using the “Normals” function (red box). The green normal areas are selected to indicate two healthy vessel segments.

2.9.2 Fixed proximal reference

To impute a reference size for a particular segment use the fixed reference tool. Select “Fixed prox” under the “Check reference” (text fig 13, red box). A fixed proximal reference size is selected with a 0.25 mm interval from 2 to 5 mm. Place the proximal green marker where the vessel should

have the indicated value. A normal distal area is chosen to adjust the slope of the linear function (see fig. 13).

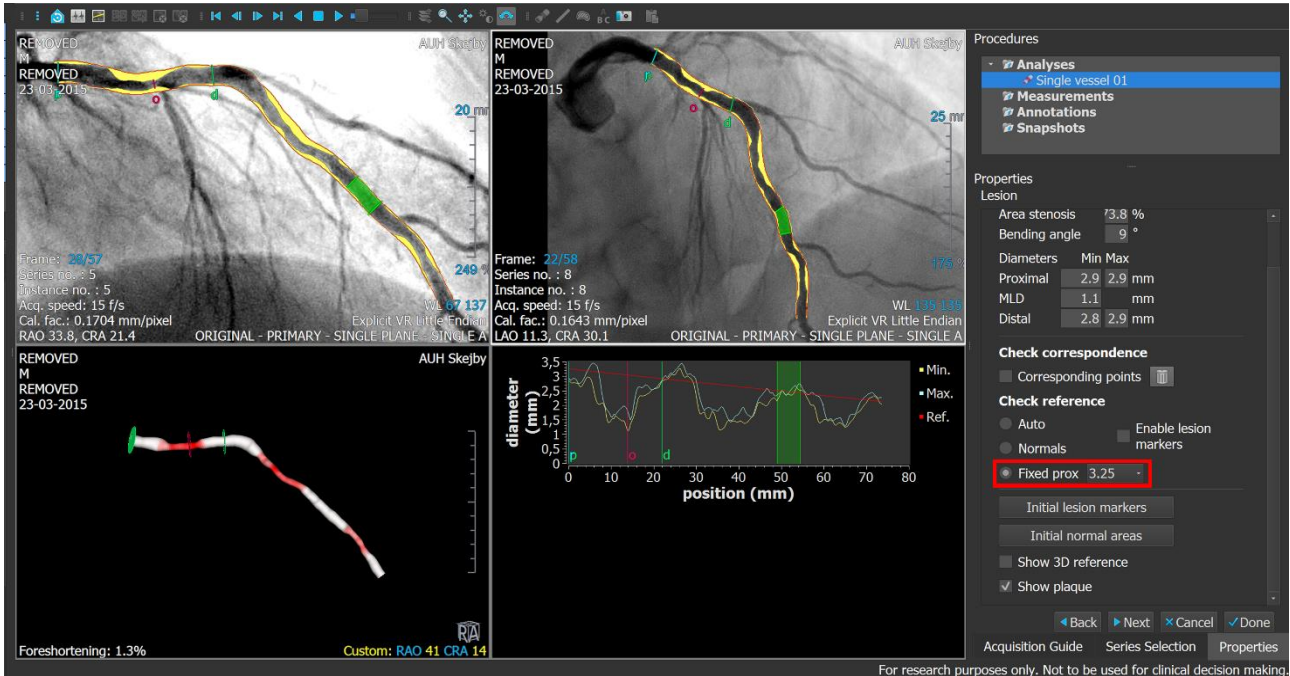


Figure 13 Reference function editing using the "Fixed Prox" function (red box). The normal areas is moved to indicate a healthy distal vessel segment.

2.9.3 Reference diameter strategy

If the automatic generated reference function based on the 3D-reconstruction follows the criteria (2.9), it is used as the first choice. If not satisfied, selection of normal areas (2.9.1) is recommended in vessels with:

- Clearly identifiable healthy segments
- Realistic proximal reference size of the vessel according to gender and body mass index

A fixed proximal reference (2.9.2) is recommended in cases with:

- Proximal LAD disease defined as a proximal LAD reference size < 2.5 mm for women and < 3.0 mm for men in Caucasians with healthy segments distally
- Diffuse LAD disease with segments in mid/distal vessel parts exceeding the proximal reference size

The fixed proximal diameter is set to 3.0-3.5 mm men and 2.5-3.0 mm for women depending on the size of LM and LCx) and the patient (age, MBI).

Verify the reference diameter (criteria from 2.9) by looking at the diameter graph in the lower right panel. The red line indicates the reference lumen diameter, and the two graphs the minimum and maximum lumen diameters from the two images.

NOTE: it is more **important to have a correct reference function by manual adjustments** than preserving a wrongly automatic generated reference function to aim for reduced variability

2.10 Fixed flow QFR computation

1. Press next
2. Indicate Nitro yes or no
3. Enter *Vessel segment*: Left main/LAD or Other coronary (fig 14, red box)

A Fixed Flow QFR will now be calculated

2.11 Frame count based QFR computation

For a potentially more accurate calculation of QFR, frame count based computation is performed;

1. Frame count (Figure 14, yellow box)

a. Choose projection for frame count, either

- i. The left panel run
- ii. The right panel run
- iii. Another projection

The projection in which frames are counted should show good contrast filling, have a constant contrast flow/speed, a frame rate of at least 12.5 frames/sec for contrast QFR and 25 frames/sec for adenosine QFR.

b. *Start frame* is indicated as the frame in which the contrast arrives at the proximal pathline point

c. *End frame* is indicated as the frame in which the contrast arrives at the distal pathline point

d. If the proximal or distal point pathline is reached by the contrast between two frames, the first of the two frames is chosen, and the $+1/2$ -box is ticked off

e. Another option is to relocate the proximal and the distal vessel delimiters, to get a better correspondence between the chosen start or end frame and the contrast position

PLEASE NOTE that projections where the contrast seems to appear uniformly in most of the analysed segment simultaneously are not appropriate for frame count. Remember to enter patient state (the angiographic run for frame counting is acquired during resting condition or hyperaemia).

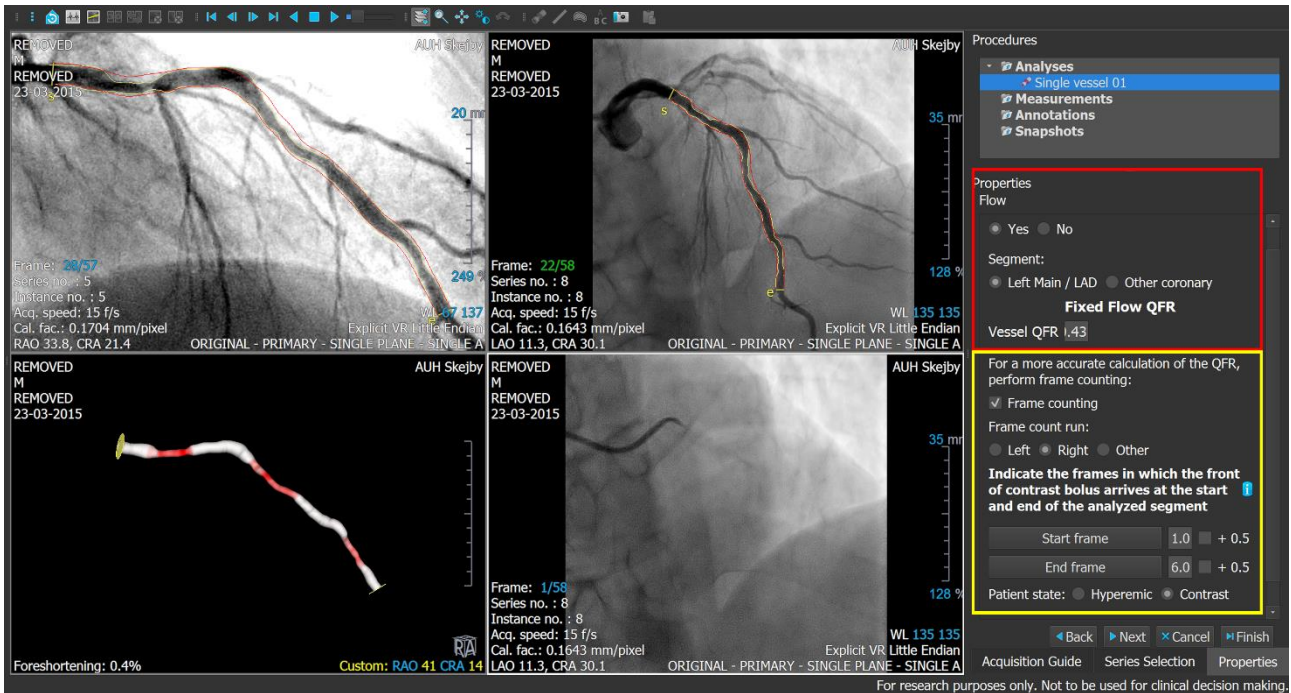


Figure 14 Red box: indicate vessel for fixed flow QFR computation. Yellow box: Frame count QFR analysis by indicating the start- and end frame for contrast flow through the segmented vessel part. Frames are found by scrolling through the selected run in lower right image panel.

After frame count QFR is calculated the following QFR-values are listed (fig 15):

- Lesion QFR: calculated for the lesion segment between the two green lesions markers. Segments proximal to the proximal lesion marker are considered non-stenotic
- Vessel QFR: calculated for the entire contoured segment. Segments proximal to the contoured segment are considered non-stenotic
- Index QFR: calculated from the proximal end of the contoured segment to the user defined white index line. The index line can be moved within the contoured vessel segment. When comparing QFR and FFR directly, make sure to place the index line at the site of the

pressure transducer on the pressure wire. To identify the wire position, choose 'View'-state and identify the wire position.



Figure 15 QFR results (red box).

2.12 Documentation

After finalizing analysis, it is saved by two steps for the study purpose.

1. A screenshot is acquired and saved in a folder named "Patient X", X indicating the patient's study ID. The screenshot should be of the entire screen including the time and date in lower right corner of Windows
2. The QFR analysis is saved in the Medis Suite QAngio XA 3D/QFR solution by clicking *Done* in the lower right corner and clicking save as in the upper panel to save with study ID (Figure 16, red marker)



Figure 16 Documentation. How to save the analysis in the Medis Suite QAngio XA 3D/QFR solution.

- After an analysis is finalized, Medis Suite QAngio XA 3D/QFR solution creates a report summarizing the analysis, including 2D images of the vessel reconstruction, the 3D reconstruction, results and more (fig. 17).

Spacex OU

Medis Suite 2.1 Report

Organization: Your organisation name (in configuration) REMOVED: REMOVED
Report created by: Jelmer Sybren
Report date/time: 09-02-2017 15:47
Session name: Session 09-02-2017 11:16 Jelmer Sybren_CASETILSOP (Unsaved)

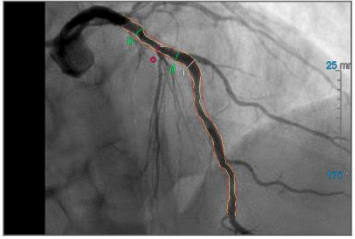
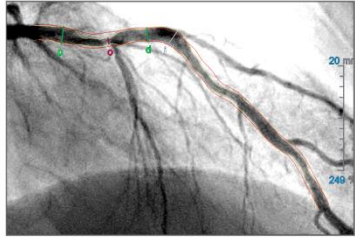
Patient Study Info

Name:	REMOVED	Study date:	23-03-2015
ID:	REMOVED	Description:	KFNG Udvidelser og rekanaliseringer af kor-a.
Birthdate:		Accession number:	REMOVED
Age/Gender:	-/M	Referring physician's name:	
Modality:	XA	Institution name:	AUH Skejby
Manufacturer:	Philips Medical Systems	Performing physician's name:	AARØ^JENS^^^
Manufacturer model:	AlluraXper	Operator's name:	
		Acquisition number:	

Reason for Referral F-rlit

Single vessel 01 (QAngio XA 3D 1.1 #1) - Research only / not for clinical use

Calibration Factor:	0.1704 mm/pixel	Calibration Factor:	0.1643 mm/pixel
Source:	Isocenter calibration	Source:	Isocenter calibration



2D Image 2D Image

Browser View QAngio XA 3D 1.1 #1 Report


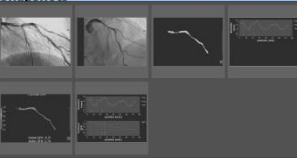
Report

Snapshots


Figure 17 Report. Access the report by selecting the Report pane (red box).

3. Specific lesion subsets

Left main coronary artery (LMCA)

- Stenosis in LMCA can only be assessed if the aorto-ostium is not involved (see 1.1)
- QFR of LMCA stenosis in combination with proximal Cx stenosis is not recommended with the present version of QFR (see 1.5)

Ostial stenosis in Cx or SBs with healthy main vessel but large diameter difference

- See 1.5 if the main vessel is diseased, otherwise the following applies:
 - The ostium must be visible in both angiographic views to be able to segment the entire stenosis
 - The proximal marker should be placed in the ostium
 - It is important to optimize the size of the reference diameter. In most cases, reference diameter editing is required (2.8.1 + 2.8.2) to ensure tapering of the reference diameter.

Left main coronary artery (LMCA) + Left anterior descending artery (LAD)

- If a stenosis is present in both the LMCA and LAD, it is important to place the proximal point in the LMCA, proximal to both stenoses

Left anterior descending artery (LAD)

- In QFR analysis of a proximal LAD stenosis in combination with a healthy LMCA, consider to use reference function editing to ensure a fitting to the LAD reference diameter (2.8.1 + 2.8.2)

Table S1. Analysis strategy.

		Definition
Primary comparison	Sensitivity and specificity of QFR compared to % DS 2D-QCA with FFR as reference	Sensitivity: proportion of true positives. Specificity: proportion of true negatives. QFR and FFR cut-point: ≤ 0.80 . Percent DS = $\leq 50\%$
Key secondary analysis	Feasibility	Fraction of lesions with successful FFR measurements where QFR is computed
	Time to QFR	Time from start of frame selection for 3D-reconstruction until QFR based on contrast flow is obtained
	Time to FFR	From introducing the pressure wire in the guiding catheter until verification of drift within limits
	QFR limits to model a QFR-FFR hybrid approach	QFR values to yield a sensitivity and specificity $> 90\%$ and QFR limits to yield a sensitivity and specificity $> 95\%$

QFR indicates quantitative flow ratio; %DS: percent diameter stenosis; 2D-QCA: two-dimensional quantitative coronary angiography and FFR indicates fractional flow reserve.

Table S2. Inclusion and exclusion criteria.

	Inclusion criteria	Exclusion criteria
Patient specific	Stable angina pectoris or secondary evaluation of non-culprit lesion after acute MI	Severe asthma or severe chronic obstructive pulmonary disease
	Age ≥ 18	Acute MI < 72 hours
	Able to provide written informed consent	Severe heart failure (NYHA ≥ III)
		S-creatinine > 150 µmol/L
		Allergy to contrast media or adenosine
		Atrial fibrillation
Angiographic	Diameter stenosis 30-90% by visual estimation	Aorta-ostial stenosis
	Reference vessel size > 2.0 mm in stenosed segment	Bifurcation stenosis with lesions on both sides of a major shift (>1mm) in reference diameter
		Poor image quality precluding contour detection
		Good contrast filling not possible
		Severe overlap over stenosed segments
		Severe tortuosity of target vessel

MI indicates myocardial Infarction and NYHA indicates York Heart Association Functional Classification.

Table S3. Recommended angulations.

Vessel/Bifurcation	1st View	2nd View
LM+LAD/LCX	RAO 20, Caudal 45	AP, Caudal 10
LAD/Diag	AP, Cranial 45	RAO 35, Cranial 20
LCX/OM	LAO 10, Caudal 25	RAO 25, Caudal 25
Proximal and mid RCA	LAO 45, Caudal 0	AP, Caudal 0
PLA/PDA	LAO 45, Caudal 0	LAO 30, Caudal 30

Table S4. Number of included patients per site.

Site	Included patients	Patients in analysis
Skejby	116	94
Essen	5	5
Ferrara	48	37
Mestre	5	4
Caserta	16	12
Hague	21	18
Gifu	44	42
Warsaw	36	35
Madrid	12	12
Naples	18	13
Giessen	8	0
Total	329	272

Table S5. Diagnostic accuracy.

A

QFR	FFR		
	<=0.80	>0.80	
<=0.80	90	28	118
>0.80	14	185	199
	104	213	317

2D-QCA	FFR		
	<=0.80	>0.80	
>=50% DS	46	50	96
<50% DS	58	163	221
	104	213	317

B

QFR	FFR		
	<=0.80	>0.80	
<=0.80	86	28	114
>0.80	17	141	158
	103	169	272

2D-QCA	FFR		
	<=0.80	>0.80	
>=50% DS	42	44	86
<50% DS	61	125	186
	103	169	272

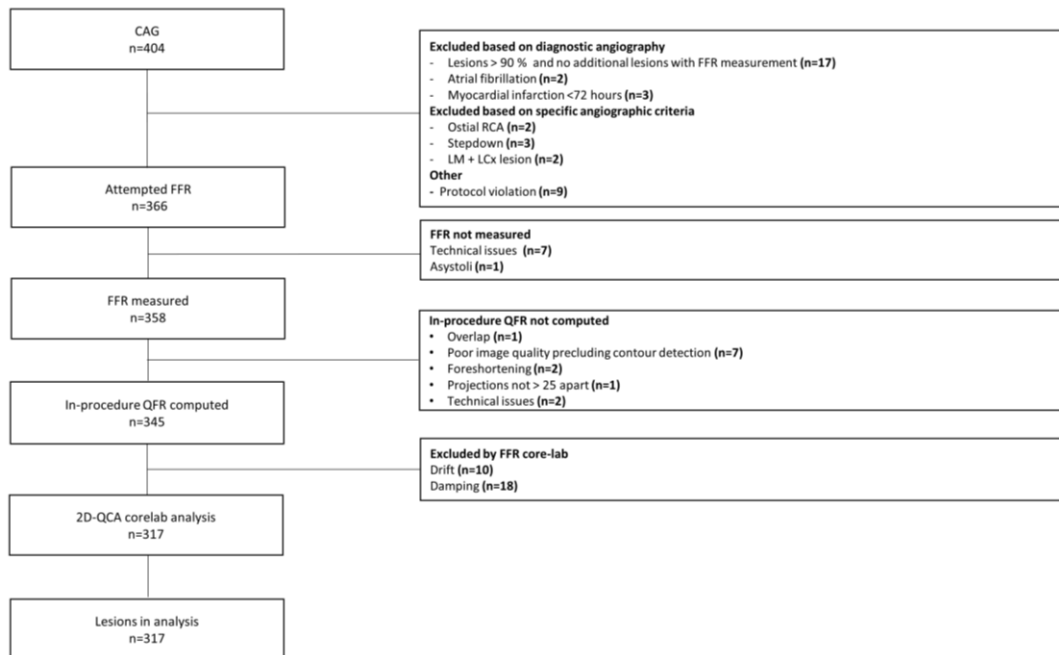
2*2 tables for QFR vs. FFR and QFR vs. 2D-QCA on per-vessel level **(A)** and per-patient level **(B)**.

Table S6. Predictors of QFR-FFR discrepancy.

	Multilevel mixed-effect model		Absolute QFR-FFR difference		p	Correlation	
	Odds Ratio	P	Yes	No		Spearman	p
Diabetes	2.88 (95%CI: 1.30-6.43)	0.01	0.03 (IQR: 0.02-0.05)	0.03 (IQR: 0.02-0.07)	0.06		
Smoking	0.44 (95%CI: 0.18-1.03)	0.06	0.03 (IQR: 0.01-0.05)	0.03 (IQR: 0.02-0.06)	0.09		
% DS (2D-QCA)	1.02 (95%CI: 0.98-1.06)	0.23				0.07	0.18

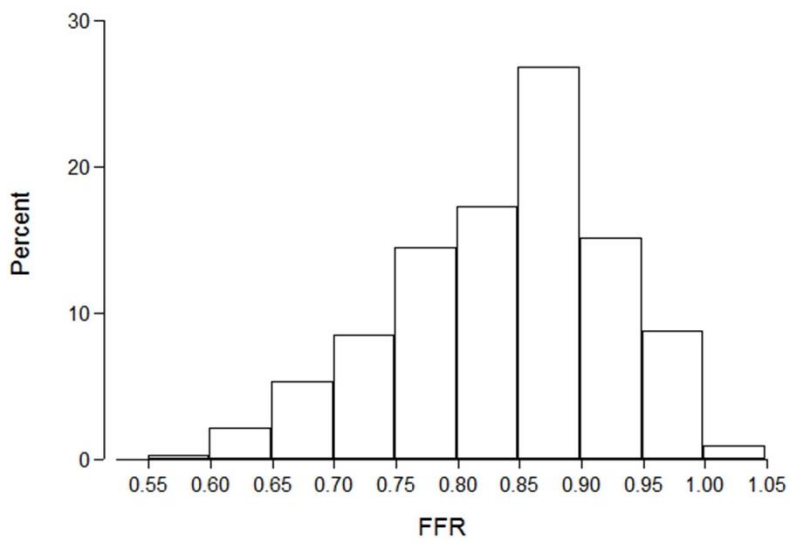
% DS indicates percent diameter stenosis and 2D-QCA indicates two-dimensional diameter stenosis

Figure S1. Vessel-level flowchart.



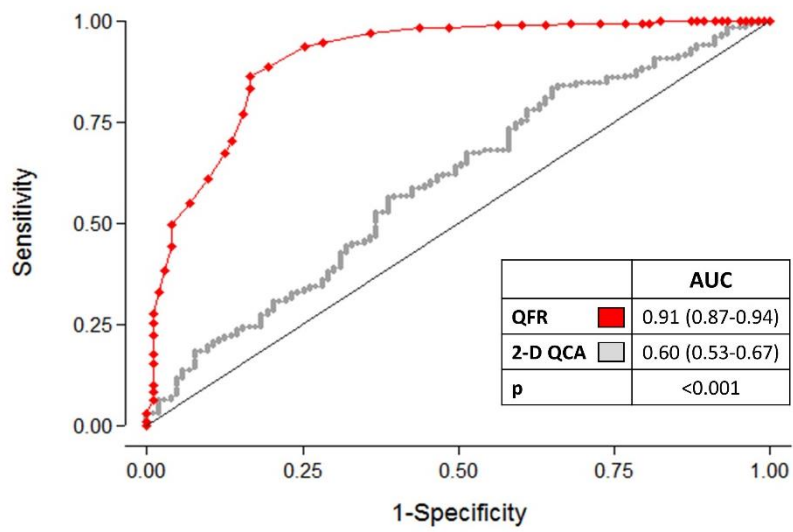
n indicates number of vessel; FFR: fractional flow reserve; RCA: right coronary artery; QFR: quantitative Flow ratio and QCA indicates quantitative coronary angiography.

Figure S2. FFR distribution.



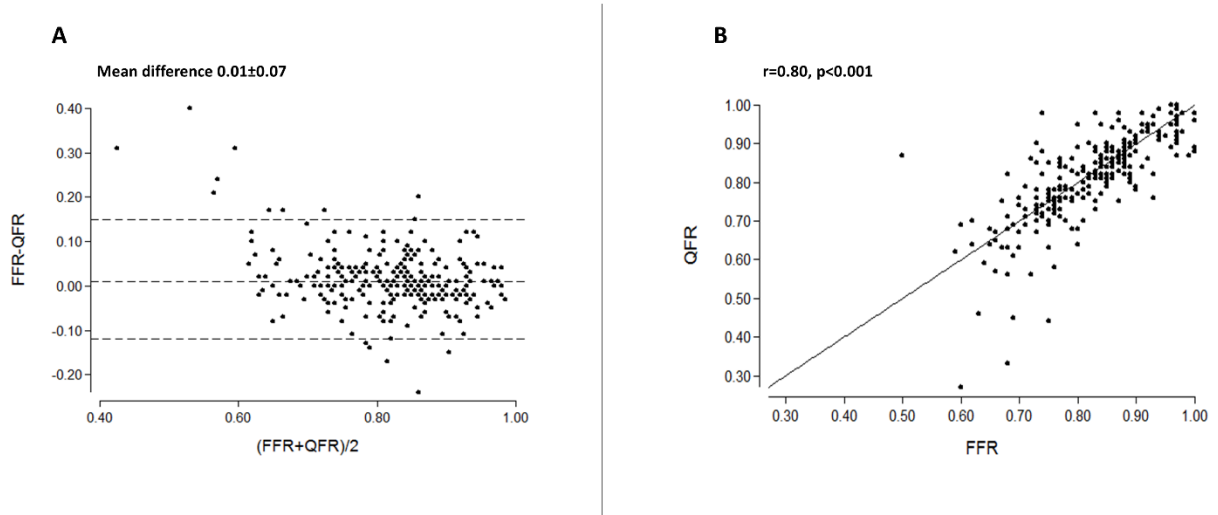
Disease severity according to fractional flow reserve (FFR). Mean FFR was 0.83 ± 0.09 and 101 (32%) lesions were in the 0.75-0.85 interval.

Figure S3. Per-patient level diagnostic performance.



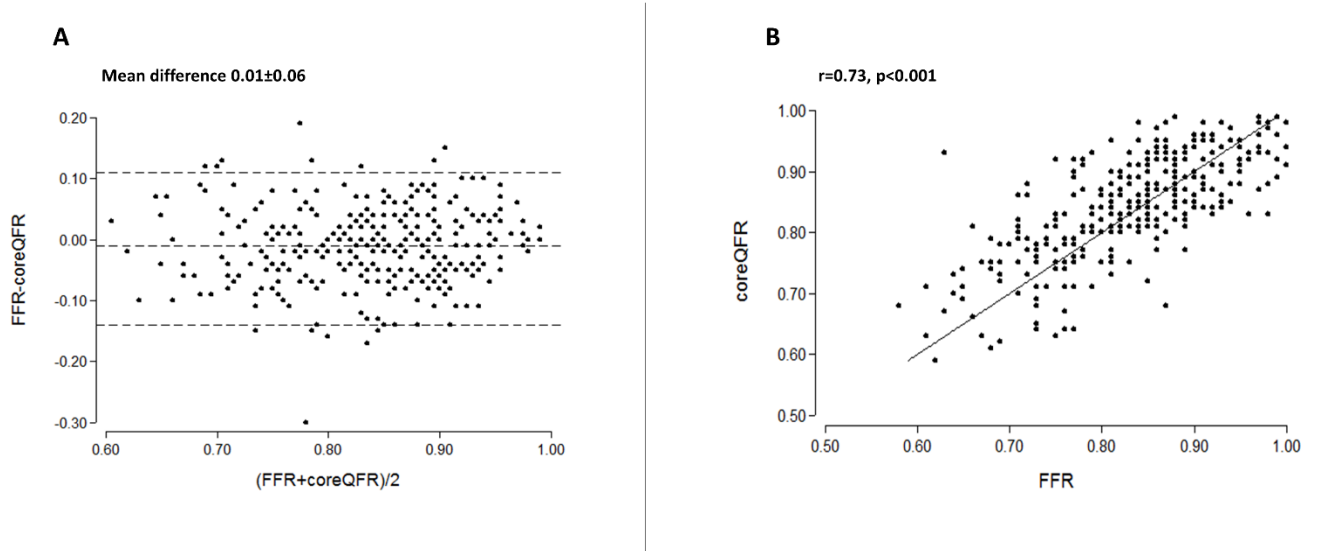
Comparison of quantitative flow ratio (QFR) and two-dimensional quantitative coronary angiography (2D-QCA) using $FFR \leq 0.80$ as reference. AUC indicates area under the receiver curve.

Figure S4. Per-patient level correlation and agreement of QFR and FFR.



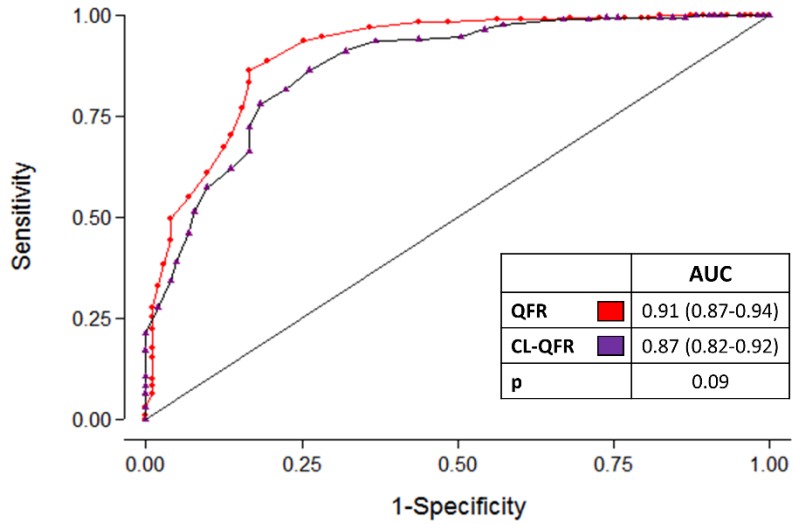
Good per-patient correlation **(A)** and agreement **(B)** of QFR and FFR was observed. Dashed lines in Bland-Altman plot illustrate mean difference ± 2 SD. QFR indicates quantitative flow ratio and FFR indicates fractional flow reserve.

Figure S5. Core-lab QFR correlation and agreement with FFR.



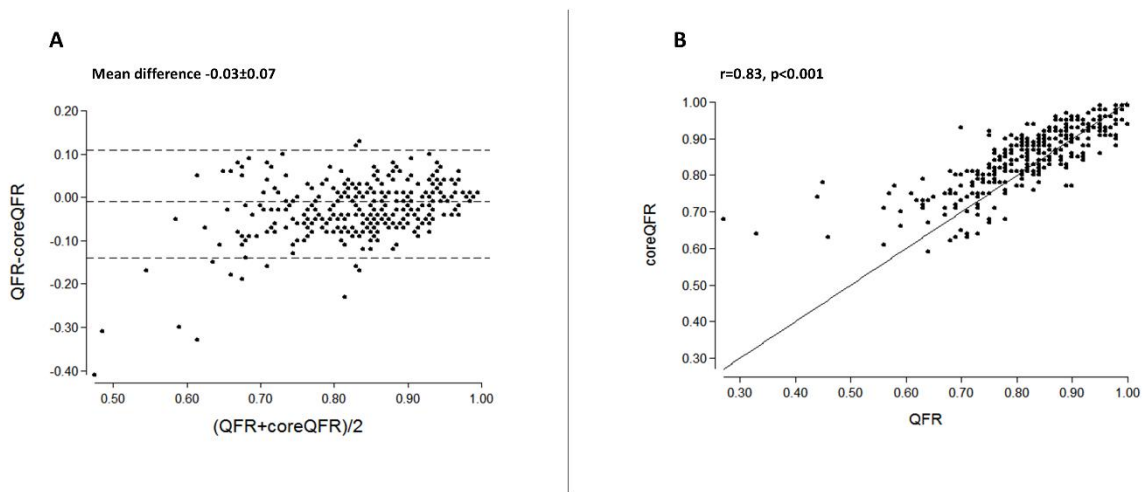
Good correlation **(A)** and agreement **(B)** of between core-lab QFR and FFR was observed. Dashed lines in Bland-Altman plot illustrate mean difference ± 2 SD. QFR indicates quantitative flow ratio and FFR indicates fractional flow reserve.

Figure S6. Per-patient level diagnostic performance of corelab-QFR and in-procedure QFR.



Comparison of in-procedure quantitative flow ratio (QFR) and corelab QFR using $FFR \leq 0.80$ as reference. AUC indicates area under the receiver curve.

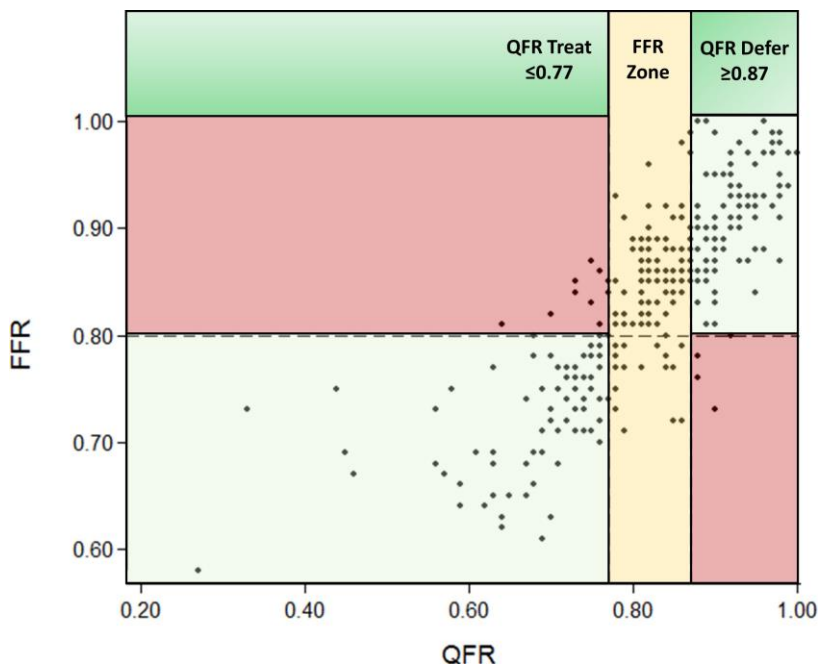
Figure S7. Correlation and agreement of corelab-QFR and in-procedure QFR.



Good correlation **(A)** and agreement **(B)** of in-procedure QFR and corelab QFR was observed.

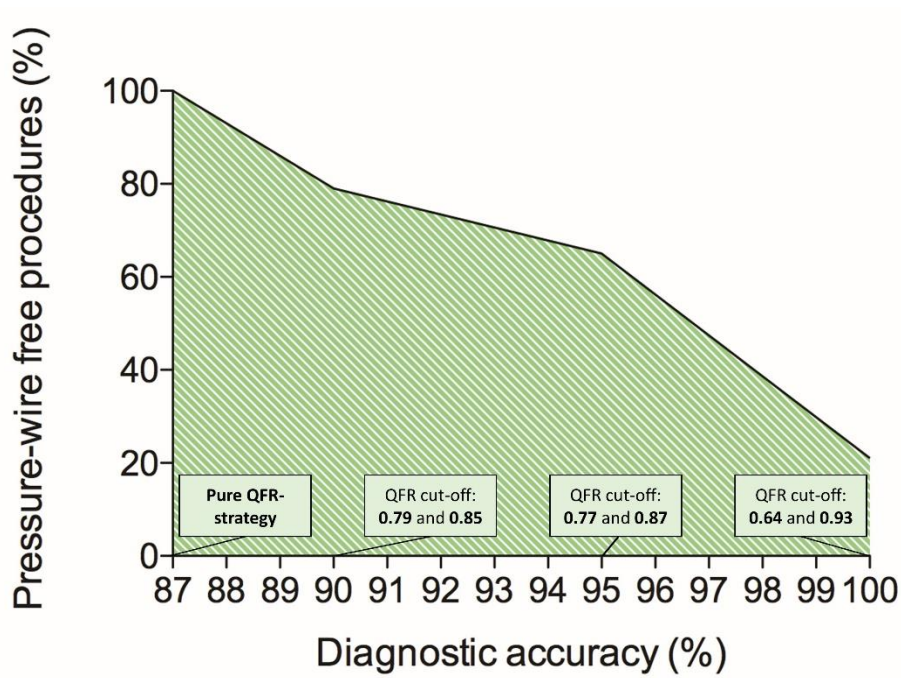
Dashed lines in Bland-Altman plot illustrate mean difference ± 2 SD. QFR indicates quantitative flow ratio and FFR indicates fractional flow reserve.

Figure S8. Clinical application of QFR.



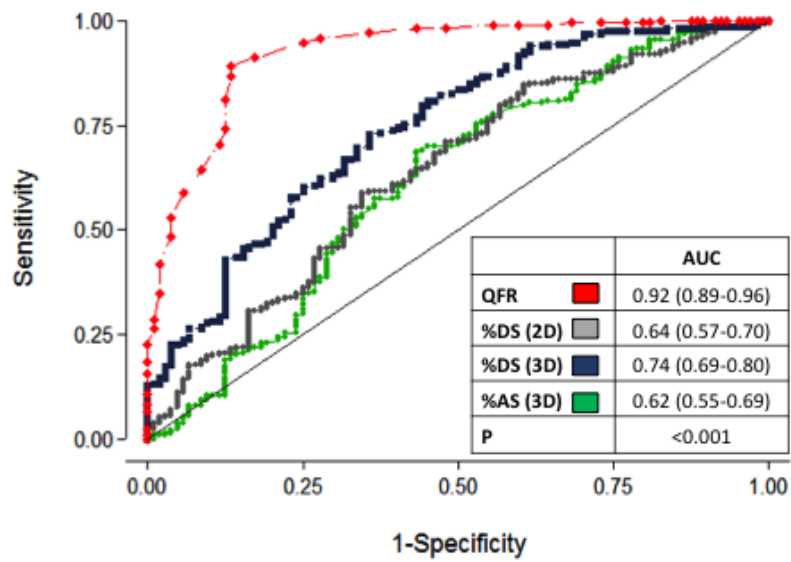
QFR limits to achieve $\geq 95\%$ sensitivity (QFR-treat 0.77) and $\geq 95\%$ specificity (QFR-defer 0.87) were identified for use in a QFR-FFR hybrid approach. QFR indicates quantitative flow ratio and FFR indicates fractional flow reserve.

Figure S9. QFR-FFR hybrid strategy.



The diagnostic agreement between FFR and QFR increases with adjusted QFR-treat and QFR-defer limits. With increasing diagnostic agreement, fewer lesions are evaluated without pressure-wires and adenosine. This analysis assumes that FFR is 100% accurate. QFR indicates quantitative flow ratio.

Figure S10. Per-vessel level diagnostic performance of in-procedure QFR, 3D-QCA and 2D-QCA.



Comparison of in-procedure quantitative flow ratio (QFR), 2D-QCA and 3D-QCA using $FFR \leq 0.80$ as reference. AUC indicates area under the receiver curve; %DS: percent diameter stenosis and %AS indicates percent area stenosis.